Environment International 156 (2021) 106730

Contents lists available at ScienceDirect

Environment International

journal homepage: www.elsevier.com/locate/envint

Alternatives for the worse: Molecular insights into adverse effects of bisphenol a and substitutes during human adipocyte differentiation

Alexandra Schaffert [a,1], Laura Krieg [a,1], Juliane Weiner [b,c], Rita Schlichting [d], Elke Ueberham [e], Isabel Karkossa [a], Mario Bauer [f], Kathrin Landgraf [g], Kristin M. Junge [f], Martin Wabitsch [h], Jörg Lehmann [e], Beate I. Escher [d,i], Ana C. Zenclussen [f], Antje Körner [g], Matthias Blüher [b,c], John T. Heiker [b], Martin von Bergen [a,j], Kristin Schubert [a,*]

[a] Department of Molecular Systems Biology, Helmholtz Centre for Environmental Research (UFZ), Leipzig, Germany
[b] Helmholtz Institute for Metabolic, Obesity and Vascular Research (HI-MAG), Leipzig, Germany
[c] Department of Endocrinology, Nephrology Rheumatology, University Hospital Leipzig Medical Research Center, Leipzig, Germany
[d] Department of Cell Toxicology, Helmholtz Centre for Environmental Research (UFZ), Leipzig, Germany
[e] Department of Therapy Validation, Fraunhofer Institute for Cell Therapy and Immunology, Leipzig, Germany
[f] Department of Environmental Immunology, Helmholtz Centre for Environmental Research (UFZ), Leipzig, Germany
[g] Center for Pediatric Research, Hospital for Children & Adolescents, University of Leipzig, Leipzig, Germany
[h] Division of Pediatric Endocrinology and Diabetes, Ulm University Medical Center, Ulm, Germany
[i] Environmental Toxicology, Center for Applied Geoscience, Eberhard Karls University Tübingen, Germany
[j] Institute of Biochemistry, Leipzig University, Leipzig, Germany

ARTICLE INFO

Handling Editor: Heather Stapleton

Keywords:
Peroxisome proliferator-activated receptor γ (PPARγ)
Bisphenol A (BPA)
Endocrine disruption
Obesogene
SGBS
Proteomics

ABSTRACT

Bisphenol A (BPA), which is used in a variety of consumer-related plastic products, was reported to cause adverse effects, including disruption of adipocyte differentiation, interference with obesity mechanisms, and impairment of insulin- and glucose homeostasis. Substitute compounds are increasingly emerging but are not sufficiently investigated. We aimed to investigate the mode of action of BPA and four of its substitutes during the differentiation of human preadipocytes to adipocytes and their molecular interaction with peroxisome proliferator-activated receptor γ (PPARγ), a pivotal regulator of adipogenesis. Binding and effective biological activation of PPARγ were investigated by surface plasmon resonance and reporter gene assay, respectively. Human preadipocytes were continuously exposed to BPA, BPS, BPB, BPF, BPAF, and the PPARγ-antagonist GW9662. After 12 days of differentiation, lipid production was quantified via Oil Red O staining, and global protein profiles were assessed using LC-MS/MS-based proteomics. All tested bisphenols bound to human PPARγ with similar efficacy as the natural ligand 15d-PGJ2 *in vitro* and provoked an antagonistic effect on PPARγ in the reporter gene assay at non-cytotoxic concentrations. During the differentiation of human preadipocytes, all bisphenols decreased lipid production. Global proteomics displayed a down-regulation of adipogenesis and metabolic pathways, similar to GW9662. Interestingly, pro-inflammatory pathways were up-regulated, MCP1 release was increased, and adiponectin decreased. pAKT/AKT ratios revealed significantly reduced insulin sensitivity by BPA, BPB, and BPS upon insulin stimulation. Thus, our results show that not only BPA but also its substitutes disrupt crucial metabolic functions and insulin signaling in adipocytes under low, environmentally relevant concentrations. This effect, mediated through inhibition of PPARγ, may promote hypertrophy of adipose tissue and increase the risk of developing metabolic syndrome, including insulin resistance.

1. Introduction

The World Health Organization (WHO) reports that in 2016 nearly 40% of the adult world population were overweight and 13% obese with some countries reaching overweight rates of up to 70% and obesity rates of nearly 40% (WHO 2020). Besides hypercaloric nutrition and low

* Corresponding author at: Department of Molecular Systems Biology, Helmholtz Center for Environmental Research, Permoserstraße 15, 04318 Leipzig, Germany.
E-mail address: kristin.schubert@ufz.de (K. Schubert).
[1] These authors contributed equally to this work.

https://doi.org/10.1016/j.envint.2021.106730
Received 21 January 2021; Received in revised form 16 June 2021; Accepted 17 June 2021
Available online 27 June 2021

physical activity, it has been suggested that environmental contaminants acting as endocrine disruptors play a crucial role in accelerating the obesity pandemic (Legeay and Faure, 2017; Darbre, 2017). Among the most discussed obesogenic compounds is bisphenol A (BPA). BPA is a component in the manufacturing of polycarbonate plastic and epoxy resin linings of food and drinking cans. Hence, human exposure can occur on a daily basis, mainly through dietary intake, but also by air and dust, cosmetics, toys, and skin contact (ANSES 2014). Due to the ubiquitous usage of BPA and, consequently, substantial exposure to it, the compound is not only present in the environment but has also been detected in human serum in concentrations ranging from 0.0002 to 66 ng/ml (Legeay and Faure 2017). Unfortunately, BPA exposure is also associated with reproductive diseases, increased risk of cancer, and developmental impairment (Acconcia, Pallottini, and Marino 2015). In recent years, industries started to substitute BPA due to restrictions by several regulatory authorities (ECHA). These substitute compounds often include BPA analogs, e.g., Bisphenol AF (BPAF), Bisphenol B (BPB), Bisphenol F (BPF), and Bisphenol S (BPS). However, similarities in the chemical properties of BPA and its substitutes suggest that they also possess endocrine disruptive properties and raise questions about their suitability as safer substitute compounds.

Over the last two decades, BPA has been repeatedly linked to obesity and an increased risk for metabolic diseases in studies in vivo, causing weight gain and impaired glucose tolerance in mice (Miyawaki et al. 2007; Wei et al. 2011; Ding et al. 2014). In vitro, BPA has been shown to promote adipogenesis and lipid accumulation in human and mouse adipocytes with alterations in lipid metabolism in μM concentration ranges (Ohlstein et al. 2014; Masuno et al. 2005; Helies-Toussaint et al. 2014; Martinez et al. 2020). Additionally, many in vivo as well as in vitro studies have demonstrated altered apolipoprotein and adipokine expressions upon exposure to BPA, suggesting adipose tissue dysfunction (Hugo et al. 2008; Ariemma et al. 2016; Wang et al. 2018; Ivry Del Moral et al. 2016). On the contrary, De Filippis, Li, and Rosen (2018) did not find an enhancing effect of BPA on adipogenesis but detected decreased insulin sensitivity and a pro-inflammatory effect, thus potentially contributing to the development of the metabolic syndrome.

Missing consensus on the impact of BPA and underlying molecular mechanisms, including the interaction with peroxisome proliferator-activated receptor γ (PPARγ)), which plays a pivotal role in the regulation of adipogenesis and adipose tissue functions, still creates considerable ambiguity in the mode of action in adipose tissue. Ahmed and Atlas (2016) have demonstrated a link between adipogenesis-promoting effects of BPA and direct activation of PPARγ, that has previously been identified as a target for metabolic disruption (Le Magueresse-Battistoni et al. 2017). Contrary to that, others did not detect PPARγ-activation through BPA and argue that the acceleration of adipogenesis through bisphenols happens through a so far unknown PPARγ-independent pathway (Chamorro-García et al. 2012; Riu et al. 2011).

BPA substitutes are not sufficiently investigated for adverse effects and obesogenic properties in particular (Thoene et al. 2020). Some studies found similar differentiation-promoting effects for BPA alternatives BPS, BPB, BPE, and BPF in high concentrations (Wang et al. 2018; Masuno et al. 2005; Ahmed and Atlas 2016; Boucher, Ahmed, and Atlas 2016).

Therefore, the primary purpose of this paper was to investigate the possible metabolic disruptive properties of the emerging BPA substitutes, which are up to date not well studied, and compare them to BPA for which adverse effects have been described before (Ohlstein et al. 2014; Masuno et al. 2005; Helies-Toussaint et al. 2014; Martinez et al. 2020). We aimed to reveal the molecular mechanisms behind their effects on humans, in contrast to the more often investigated metabolic disruptive endpoints like lipid accumulation and PPARγ agonism and commonly used mouse adipocyte cell lines (Ahmed and Atlas 2016; Masuno et al. 2005). Therefore, we used Omics in addition to classical endpoints to reveal mechanistic insights in human adipocytes. We focused on the involvement of PPARγ since it is a master regulator of adipogenesis, and data on its involvement is lacking for almost all BPA substitutes.

To unravel their effects on adipogenesis, human preadipocytes (Simpson-Golabi-Behmel Syndrome (SGBS) cells), derived from subcutaneous adipose tissue, were exposed to BPA and its emerging substitutes BPB, BPF, BPAF, and BPS during the differentiation. To understand the involvement of PPARγ, binding and activation of the receptor were determined for all bisphenols under consideration of cell viability. Systemic biological effects of BPA and its substitutes were analyzed using global proteomics. The release of adipokines, insulin sensitivity, and oxidative stress parameters were compared, giving insights into adipocyte function.

2. Materials and methods

2.1. Chemicals

All reagents were ACS grade or higher. All solvents used were LC/MS grade. Acetonitrile (ACN), isopropanol, formic acid (FA), ethanol (EtOH), methanol (MeOH), 1,4-dithiothreitol (DTT), iodoacetamide (IAA), and triethylammonium bicarbonate buffer (TEAB, Sigma Aldrich, Germany) were obtained from Sigma-Aldrich. Ammonium bicarbonate was purchased from MP Biomedicals. Modified trypsin (sequencing grade) was obtained from Promega. TMT-10-plex kit, tris-(2-carboxyethyl)-phosphine (TCEP), and Pierce 660 nm Protein assay were used from Thermo Fisher Scientific. Rosiglitazone, BPA, BPAF, BPB, BPS, and BPF were from Sigma Aldrich, PPARγ ligand 15-deoxy-delta-12,14-prostaglandin J2 (15d-PGJ2) from Santa Cruz Biotechnology, and PPARγ-inhibitor 2-chloro-5-nitrobenzanilide (GW9662) was from Cayman Chemicals. Cell culture medium and chemicals DMEM/F12, biotin, penicillin/streptomycin, cortisol, apo-transferrin, triiodothyronine, human insulin, dexamethasone, 3-isobutyl-1-methylxanthine, sterile dimethyl sulfoxide (DMSO), and phosphate-buffered saline (PBS) were purchased at Sigma Aldrich. Fetal calf serum (FCS) was from Gibco.

2.2. Surface plasmon resonance (SPR) spectroscopy

SPR is a powerful technique previously used to determine binding efficacies of a variety of ligands to human PPARγ (van Marrewijk et al. 2016; Yu et al. 2004; Shang and Kojetin 2021) and utilized to characterize the binding of xenobiotics (Kratochvil et al. 2018). Binding efficacy can be monitored in real-time and label-free. In order to identify direct molecular binding interactions between a bisphenol and PPARγ, all five bisphenols were screened on a Biacore T200 instrument (GE Healthcare, Freiburg, Germany). The surface of an S Series Sensor Chip CM5 (GEHealthcare) was activated for immobilization with a mixture containing 50 mM N-hydroxysuccinimide (NHS) and 195.6 mM 1-ethyl-3-(3-dimethylaminopropyl)carbodiimide hydrochloride (EDC). A recombinant human PPARγ ligand binding domain (LBD) (Biozol) was immobilized on the chip surface at 25 °C via amine coupling and using a protein concentration of 80 μg/ml in 10 mM sodium acetate buffer (pH 4.5) at a flow rate of 5 μl/min according to the manufacture's protocol, leading to immobilization of 8959.4 RU. Unreacted NHS-esters were deactivated by 1 M ethanolamine- HCl (pH 8.5). The signal of an empty reference flow was subtracted from detected response signals of the cell containing the PPARγ LBD to adjust for unspecific binding to the surface. Measurements were conducted in triplicate for every analyte with four start-up buffer-injections at the beginning of each run. Raw relative responses were normalized to the molecular weight (MW, Supplementary data 7, Table A.1) of the analyte by RU/MW*100. The signal was subsequently normalized to the corresponding highest concentration of the positive control 15d-PGJ2 (endogenous PPARγ ligand), which was included in every run. A sensorgram of the quality control compound 15d-PGJ2 is provided in Supplementary data 7, Fig. A.1) Buffer injections were used as negative control and run in triplicates after start-up

injections. Raw data and normalized relative responses can be found in the supplement (Supplementary data 7, Table A.2-A.4). More details on the experimental procedure are given in our previous paper (Kratochvil et al. 2018).

2.3. Reporter gene assay

The ability of the bisphenols to biologically activate PPARγ was tested using the GeneBLAzer® PPARγ-UAS-bla 293H cell-based reporter gene assay (Invitrogen). Experiments were conducted as described previously (König et al. 2017). Briefly, agonistic activity or antagonistic activity in presence of rosiglitazone were quantified in parallel with cell viability. The PPARγ antagonists T0070907 and GW9662 as well as the compounds BPAF and BPB were dissolved in DMSO, while BPA, BPS, and BPF were dissolved in MeOH. Rosiglitazone was used as an agonistic reference compound. T0070907 and GW9662 were used as reference compounds for PPARγ antagonism (T0070907: Supplementary data 7, Fig. A.2 B). In agonistic mode, cells were incubated with either rosiglitazone or the test compounds. In antagonistic mode, cells were incubated with rosiglitazone and the test compounds simultaneously. Cells were seeded in 384-well plates at 6000 cells/well in 30 µl assay medium (phenol-red free DMEM, 2% charcoal treated fetal bovine serum, 100 U/l penicillin, and 0.1 mg/l streptomycin) and incubated for 24 h 37 °C with 5% CO_2 in 95% humidity. 10 µl of assay medium with rosiglitazone and test compounds in serial or linear dilutions were added and incubated for 22 h at 37 °C with 5% CO_2 in 95% humidity. The final rosiglitazone concentration in the antagonism assays was 5.5 nM to reach 80% of the maximum effect (EC_{80}). After the addition of 8 µl FRET detection reagent, including ToxBlazer mixture, blue and green fluorescence signals were read immediately using a 409 nm excitation filter at 460 nm and 520 nm for potential autofluorescence and again after 2 h at room temperature. PPARγ activation was determined by the ratio of blue to green FRET fluorescence signal. The signal was converted to % effect by adjusting unexposed cells that were not treated with chemical or solvent to 0% activation and the maximum effect by rosiglitazone to 100% activation. It was verified that the solvent concentrations used for the test compounds did not impact the assay. For this, serial dilutions of DMSO and MeOH stocks were assayed and found to reduce cell viability by 10% (IC_{10}) at 5.96% (v/v) (MeOH) and 1.1% (v/v) (DMSO), and a negligible effect on the GeneBLAzer® assay at the for the test compounds applied solvent concentrations (maximal 0.05% (v/v) for DMSO and 0.5% (v/v) for MeOH).

When the assay was run in antagonistic mode, a suppression ratio (SR) was calculated as previously described (Neale et al. 2017; Escher et al. 2014). A suppression ratio of 1 corresponds to a total inhibition of the activation of the assay caused by the addition of the agonist rosiglitazone. Thus, the SR 0.5, which was determined based on log-logistic concentration-effect curves, corresponds to a relative 50% reduction of the activation induced by rosiglitazone. Cell viability was calculated using cell confluency as described before (Escher et al. 2019). Confluency was detected using an IncuCyte S3 live cell imaging system (Essen BioScience, Ann Arbor, Michigan, USA). The inhibitory concentration for 10% reduction of cell viability (IC_{10}) was determined in GraphPad Prism 8 within the linear range of the concentration–response curve using the regression slope of % confluency reduction against the dosed (nominal) concentration. Only compound concentrations below the IC_{10} were included in the evaluation of PPARγ activation. In agonist mode, experiments for 15d-PGJ2 were carried out in quadruplets and experiments for the bisphenols in duplets. In antagonist mode, all assay experiments were carried out in quadruplets.

2.4. SGBS cell culture

After differentiation, human preadipocytes of the Simpson-Golabi-Behmel syndrome (SGBS) cell strain were previously shown to have high similarity to differentiated human primary preadipocytes from healthy donors with the advantage of being able to differentiate longer than primary cells (Wabitsch et al. 2001). Therefore, they were used as a cell culture model system to investigate the cellular mode of action of BPA and its substitutes during the differentiation process. SGBS cells were obtained from the laboratory of Prof. Martin Wabitsch and differentiated as described previously (Wabitsch et al. 2001). In brief, cells were maintained at 5% CO_2 and 37 °C in 95% humidity. Cells of passage 3 were grown to confluence with DMEM/F12 containing 33 µM biotin, 17 µM pantothenate, 100 U/l penicillin, and 0.1 mg/l streptomycin (basal medium) supplemented with 10% FCS. Differentiation was started (day 0) after washing cells with PBS and changing to serum-free basal medium supplemented with 0.1 µM cortisol, 0.01 mg/ml apotransferrin, 0.2 nM triiodothyronine and 20 nM human insulin (differentiation medium). Cells were differentiated for 12 days in total. For the first four days, the differentiation medium was additionally supplemented with 2 µM rosiglitazone, 25 nM dexamethasone, and 200 µM 3-isobutyl-1-methylxanthine.

For treatments with the bisphenols and the PPARγ inhibitor GW9662, differentiation media including rosiglitazone were additionally supplemented with 10 nM, 100 nM, 1 µM, or 10 µM of BPA, BPAF, BPB, BPF, BPS or GW9662 dissolved in sterile DMSO, to a final and uniform DMSO amount of 0.01% (v/v) in each treatment from day 0 to day 12. As an untreated control, differentiation with differentiation medium including rosiglitazone and containing equivalent amounts of vehicle solvent DMSO (0.01%, v/v) was used. Cell culture media were renewed every second day.

2.5. Oil red O staining of SGBS cells

To visualize lipid accumulation, SGBS cells were grown in a 96 well plate as described in 2.4, and lipids were stained on day 12 of differentiation using Oil Red O (Sigma Aldrich). Cells were preserved with 4% paraformaldehyde in PBS over night at 4 °C. Prior to staining, a 0.5% (w/v) stock solution of Oil Red O in isopropanol was diluted 2:3 with water, mixed, and set aside for 10 min before it was filtered through Whatman paper. Staining was performed using 0.132 ml/cm^2 of diluted Oil Red O (42 µl per well) and incubated for 30 min. The staining solution was removed, and the cells were carefully washed three times with ddH_2O. Microscope images were taken with a 5-fold augmentation. Differentiation of cells with rosiglitazone and equivalent amounts of DMSO (0.01% v/v) as the treatments was used as a control. Experiments were carried out in triplicate.

2.6. DAPI and nile red staining of SGBS cells

To determine the cell viability by DNA content quantification, and simultaneously quantify the degree of lipid accumulation, 4,6-Diamidino-2-Phenylindole, Dihydrochloride (DAPI) and Nile Red staining were used according to Aldridge et al. (2013). In brief, SGBS cells were grown in a 96-well plate until day 12 as described in 2.4, and preserved with 4% paraformaldehyde (Sigma Aldrich) in PBS at 4 °C overnight. Cells were washed with PBS and background fluorescence was read at Ex 360/Em 480 for DAPI and Ex 485/Em 530 for Nile Red in a 5 × 5 spot pattern. PBS was removed and 100 µl 0.2% saponin, 1 µg/ml DAPI and 1 µg/ml Nile Red in PBS were added for 15 min. Cells were washed three times with PBS and the fluorescence was read as before. Experiments were performed at least in quadruplicate. Average intensities were calculated after subtracting the background fluorescence for each well. For quantification of lipid accumulation, the ratio of Nile Red to DAPI stained cells was calculated. Differentiated SGBS cells with rosiglitazone and equivalent amounts of DMSO (0.01% v/v) as the treatments was used as a control.

2.7. Sample preparation for proteomics

SGBS cells were differentiated for 12 days in a 6-well plate in

quintuplets (*dataset of adipocyte differentiation*) and quadruplets (*dataset of bisphenol effects*). For both datasets, cells were washed with PBS and harvested from each well using 100 µl lysis buffer with 6 M urea, 2 M thiourea, and freshly added protease inhibitor in 100 mM ammonium bicarbonate. The protein concentration was determined using Pierce 660 nm assay (Thermo Fisher Scientific).

Cell lysates of the *dataset of adipocyte differentiation* were prepared as described previously (Schmidt et al. 2019). In short, protein separation was performed by 1-D SDS-PAGE (Biostep, Burkhardtsdorf, Germany). Gels were stained with Coomassie Brilliant Blue R-250 dye (Thermo Fisher Scientific). In-gel proteolytic cleavage was conducted using trypsin and samples were reconstituted in formic acid (0.1%, v/v) for mass spectrometry (MS) analysis.

For the *dataset of bisphenol effects*, cell lysates were prepared using Sera-Mag SP3 beads. The workflow was adjusted based on previous publications (Hughes et al. 2019; Hughes et al. 2014; Bannuscher et al. 2020). Furthermore, tandem mass tag (TMT)-labeling (TMT-10-plex, Thermo Fisher Scientific) was used for protein quantification, because we previously demonstrated that it enables more robust identification of pathways in a toxicological context (Wang et al. 2020). In brief, for each sample, 2 µl (=20 µg) SpeedBeads™ magnetic carboxylate modified particles (SP3 beads, GE Healthcare, Germany) per sample were washed with 200 µl water, placed on a magnetic rack, and incubated for 2 min. The supernatant was then discarded, and the washing procedure was repeated twice. For each sample, 25 µg of proteins were brought to a volume of 100 µl with 100 mM TEAB, reduced with 5 µl 200 mM TCEP (37 °C, 30 min, 550 rpm) and alkylated with 5 µl of 375 mM IAA (37 °C, 30 min, 550 rpm, darkness). To force protein binding to the SP3 beads, each sample was acidified with FA (pH ~ 2), followed by the addition of ACN (50%, v/v). Afterwards, samples were transferred to the washed SP3 beads in a 96-well plate, incubated for 8 min and then placed on the magnetic rack for an additional 2 min. The supernatant was discarded and beads washed with EtOH (70%, v/v) twice and once with ACN (100%, v/v). After drying the beads for 15 min, trypsin was added to each sample (1:50 enzyme to protein ratio, 37 °C, overnight, 550 rpm). Subsequently, each sample was labeled according to the manufacturer's instructions with a protein:label ratio of 1:4 for 1 h followed by quenching with 1 µl of 5% hydroxylamine for 15 min. ACN (>95%, v/v) was added to each tube to force peptide binding to the beads. The mixture was incubated for 8 min and then placed on the magnetic rack for an additional 2 min. The supernatant was discarded and beads washed with ACN (100%, v/v) twice. Peptides were eluted in two fractions. The first fraction was gained using 87% (v/v) ACN and ammonium formate (pH 10) in water. The second fraction was eluted using water with DMSO (2%, v/v) and sonication (1 min). The tube was placed on the magnetic rack and incubated for 2 min. The supernatant containing the peptides was collected, vacuum-dried, and reconstituted in FA (0.1%, v/v) for MS analysis.

2.8. Untargeted proteomics

All samples were analyzed on a nano ultra-performance liquid chromatography (UPLC) system (Ultimate 3000, Thermo Fischer Scientific) coupled on-line to an Orbitrap mass spectrometer (Thermo Fischer Scientific) equipped with a chip-based ESI source (Nanomate, Advion,). Peptides (10 µg) were trapped on a C18 column (Acclaim PepMap 100 C18, nanoViper, 2 µm, 75 µm × 5 cm, Thermo Fisher Scientific, #164535) and separated on a reversed-phase C18 column (Acclaim PepMap 100 C18, nanoViper, 3 µm, 75 µm × 25 cm, Thermo Fisher Scientific, #164569).

Samples of the *dataset of adipocyte differentiation* were analyzed using MS parameters described previously (Schmidt et al. 2019). MS raw data were processed using MaxQuant 1.6.2.10, resulting in label free quantification (LFQ) intensities. The database search was performed using the UniprotKB/Swissprot reference proteome of *Homo sapiens* (26th of November 2018) and a false discovery rate (FDR) for peptides and proteins of 1%. Oxidation (methionine) and acetylation (protein N-termini) were used as variable modifications. Carbamidomethylation (cysteine) was set as fixed modification, and a maximum of two tryptic missed cleavages was allowed. Proteins with at least two identified peptides and at least one unique peptide were considered identified, and proteins were quantified based on the intensities of the top three identified peptides.

Statistical analysis was carried out in R-3.6.1 using the packages mixOmics (Rohart et al. 2017), limma (Ritchie et al. 2015), plyr (Wickham 2011), reshape2 (Wickham 2007), xlsx (Adrian and Cole, 2018), DEP (Zhang et al. 2018), ggsci (Nan 2018), circlize (Gu et al. 2014), calibrate (Jan 2019), ggplot2 (Wickham 2016), readxl (Wickham and Bryan, 2019), qpcR (Andrej-Nikolai 2018), splitstackshape (Ananda 2019), tidyr (Wickham, 2019), and Tmisc (Stephen 2019). LFQ data were Log2-transformed, filtered for proteins quantified at least in triplicate under at least one treatment, and variance-stabilized. The mean of each treatment was calculated and used for fold change (FC) calculations against day 0. This resulted in FCs for 4465 proteins (Supplementary data 1). Significant changes between timepoints and day 0 were calculated using Student's *t*-test with subsequent Benjamini & Hochberg adjusted ($p.adj \leq 0.05$; Supplementary data 2).

Samples of the *dataset of bisphenol effects* were analyzed using MS parameters described before, except that we selected the top 15 instead of the top 10 precursor ions of each MS1 scan for fragmentation here (Wang et al. 2020). MS raw data were processed using Proteome-Discoverer 2.4.0.350. The database search was conducted against the UniprotKB/Swissprot reference proteome of *Homo sapiens* (06th of March 2019). The resulting replicate-wise TMT-reporter ion intensity FCs of bisphenol vs control were used for subsequent analyses. Statistical analysis was also carried out in R-3.6.1 using the described packages. Data were Log_2-transformed, median-normalized, and filtered for reliably quantified proteins as described for the *dataset of adipocyte differentiation*. This resulted in FCs for 3372 proteins (Supplementary data 4). Significant changes between treatments and control were calculated using Student's t-tests ($p \leq 0.05$; Supplementary data 5).

For both datasets, the Ingenuity Pathway Analysis (IPA; Qiagen, Germany) tool was used for pathway enrichment analysis with the definition of "human" as organism, selection of "adipose tissue" and "adipocytes", and using significantly altered proteins. Benjamini & Hochberg adjusted p-values and z-scores were extracted (*dataset of adipocyte differentiation*: Supplementary data 3; *dataset of bisphenol effects*: Supplementary data 6) and used for visualizations.

MS data have been deposited to the ProteomeXchange Consortium via the PRIDE (Perez-Riverol et al. 2019) partner repository with the dataset identifier PXD023266 for the *dataset of adipocyte differentiation* and the identifier PXD023227 for the *dataset of bisphenol effects*.

2.9. pAKT/AKT western blot

Differentiating SGBS cells were exposed to 1 µM of BPA, BPAF, BPB, BPF, BPS, GW9662, or 0.01% (v/v) DMSO as a control, as described in 2.4. On the 12th day of differentiation, the supernatant was removed and replaced with serum- and insulin-free basal medium containing 1 µM bisphenol, GW9662, or 0.01% (v/v) DMSO. Cells were incubated overnight and then treated with 100 nM insulin or an equal amount of ddH_2O as an unstimulated control for 10 min. Cells were washed with PBS and harvested with lysis buffer containing 150 mM NaCl, 1% (v/v) Triton X-100, 50 mM Tris HCl pH 7,4, 0.5% (v/v) sodium deoxycholate, 0.1% sodium dodecyl sulfate (w/v), 32% HCl (w/v) in ddH_2O and 1x cOmplete Roche protease inhibitor (Sigma Aldrich, Germany). After 1 h incubation on ice, lysates were centrifuged for 15 min at 4 °C and 16000xg. Protein concentration was determined by BCA-Assay (Pierce). Total protein lysates (20 µg total protein per lane) were separated on 12% SDS-PAGE and transferred onto a nitrocellulose membrane using the tank blot method (BioRad, California, USA). Membranes were incubated in 3% BSA blocking buffer for 1 h, followed by incubation

with primary antibody overnight at 6 °C (dilution 1/1000). The following primary antibodies were used: β-ACTIN (A1978, Thermo Fisher Scientific), phospho-AKT (pAKT) Ser473 (#4060, Cell Signaling Technologies), and AKT (#4691, Cell Signaling Technologies). Immunoblots were washed with TBS-T (0.02% Tween20 in Tris-buffered saline) and incubated with HRP-coupled secondary anti-rabbit (#7074, Cell Signaling Technologies) or anti-mouse (#7076, Cell Signaling Technologies) antibody for 1 h at room temperature (dilution 1/2000). Chemiluminescence signal was detected using the G:BOX Chemi XX-9 system with GeneSys software (Syngene, Cambridge, UK). Quantification was performed using GeneTools software (Syngene).

2.10. Measurement of adipokines and cytokines

SGBS cell culture supernatants of 1 μM bisphenol and 1 μM GW9662 treatments were used to quantify the release of 13 adipokines and cytokines, using a bead-based multiplex assay (LEGENDplex™ Human Adipokine Panel, BioLegend, San Diego, CA, USA). Experiments were carried out in quintuplets. Supernatants were diluted 1:5 with assay buffer and analyzed in a flow cytometer FACS Calibur (BD Biosciences) according to the manufacturer's protocol, resulting in median fluorescence intensities (MFI) for each replicate. MFIs were interpolated using the build-in Prism GraphPad standard curve Asymmetric Sigmoidal, 5PL. Additionally, Adipsin, Leptin and MCP1 concentrations in the cell culture supernatants were determined using DuoSet ELISA kits from R&D Systems (Minneapolis, USA) according to the manufacturer's instructions. Adipokine concentrations were normalized to the protein amount in the cell lysate of the according well determined by BCA-Assay (Pierce).

2.11. DCFDA assay for reactive oxygen species (ROS) measurement

To analyze intracellular ROS levels, SGBS cells were seeded into a 96-well plate and differentiated until day 12 under the exposure of bisphenols as described in 2.5. ROS were quantified using DCFDA Cellular ROS Detection Assay (Abcam) according to the manufacturer's protocol. Treatments were performed in quadruplets and undyed cells were used as blank.

2.12. Statistical analysis

With the exception of the proteomics data evaluation, all other data were expressed as means ± standard deviation (SD) and analyzed via one-way or two-way ANOVA, including Dunnett's or Fishers LSD post-hoc tests or t-tests using GraphPad Prism 8 Software (La Jolla, CA, USA).

3. Results

3.1. PPARγ binding and effects on activation

PPARγ regulates key functions of the adipose tissue, including adipogenesis, lipid metabolism, and inflammation (Lefterova et al. 2014). To determine whether the bisphenols act through an interaction with it, binding and subsequent activation of PPARγ were analyzed. SPR was used to test the relative binding strength of BPA and its analogs to the human recombinant PPARγ LBD. Although SPR is a fast and reliable method for determining protein–ligand interactions, its sensitivity is rather low, creating the need to test higher concentrations (Yuk et al. 2006). All bisphenols displayed significant binding to PPARγ compared

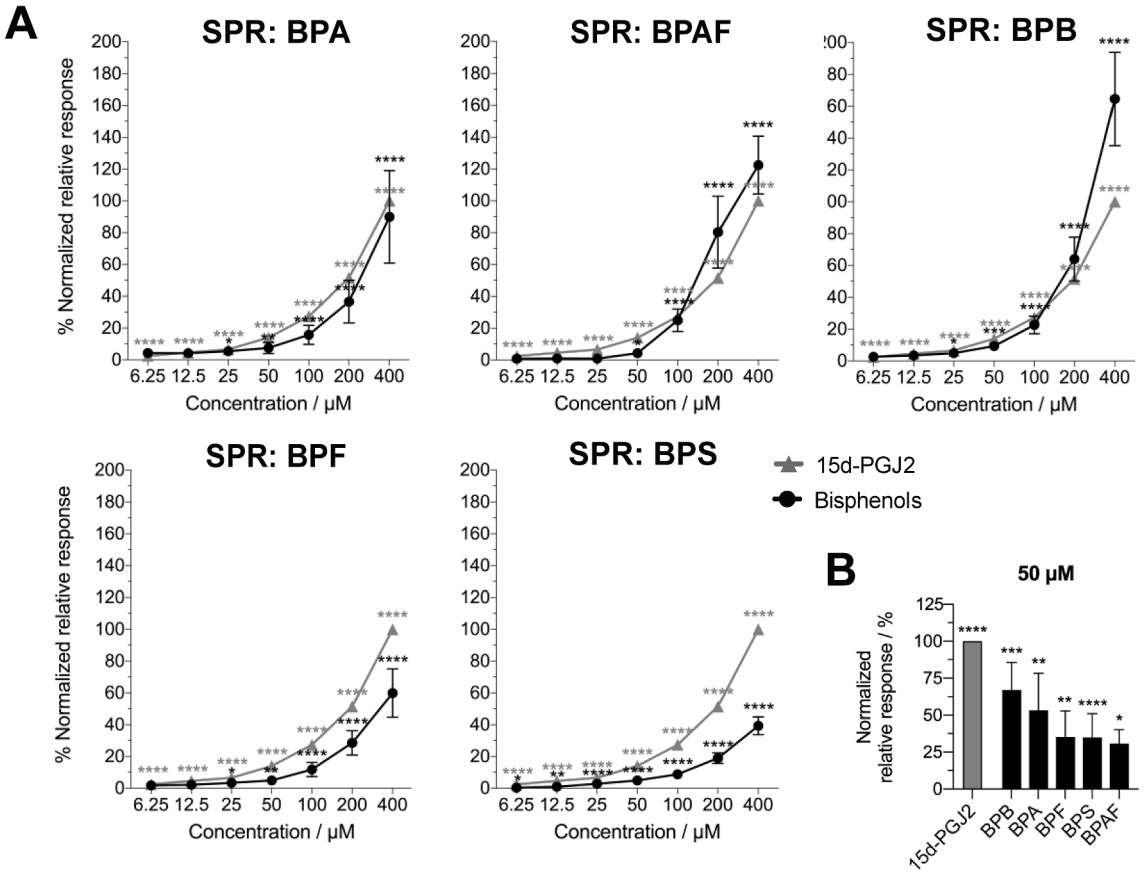

Fig. 1. Binding of bisphenols to human PPARγ. (A) SPR measurement: Relative binding responses for BPA, BPAF, BPB, BPF, and BPS normalized to the molecular weight, with the natural PPARγ ligand 15d-PGJ2 serving as the positive control. (B) Comparison of relative normalized responses at an analyte concentration of 50 μM. All plots show mean ± SD. Statistically significant differences against negative controls (running buffer injections) are indicated by asterisks (* $p \leq 0.05$, ** $p \leq 0.01$, *** $p \leq 0.001$, **** $p \leq 0.0001$).

to the negative control (Fig. 1 A). Most BPA substitutes bound with at least similar, for BPB even higher, affinity to PPARγ as BPA (Fig. 1 A). Although high μM concentrations are not environmentally relevant, these were tested in order to reach a saturation of the binding signal. Nonetheless, a saturation could not be reached for up to the maximal applied dose of 400 μM. It has to be noticed that other compounds from the group of plastic additives, which were analyzed in parallel, did not exhibit binding to PPARγ LBD (data not shown). Thus, we consider the obtained results definite.

Since 50 μM was the lowest concentration to yield significant binding signals for all bisphenols, relative responses at this concentration were compared (Fig. 1 B) and revealed the following affinity order (strongest to weakest binding efficacy is presented as follows): 15d-PGJ2 > BPB > BPA > BPF > BPS > BPAF.

To investigate if the observed binding of bisphenols to PPARγ results in its activation, the cell-based GeneBLAzer® assay was performed. The quality control compound rosiglitazone exhibited consistent activation of PPARγ and resulted in an EC_{50} of 2.3 nM, while having no toxic effects under the tested concentrations (Supplementary data 7, Fig. A.2 A). 15d-PGJ2 activated PPARγ with an EC_{50} of 650 nM and exhibited no decrease in cell viability up to 1 μM (Supplementary data 7, Fig. A.3). The bisphenols provoked a 10% decrease in cell viability (IC_{10}) that was within the predictions for baseline cell viability decrease (toxic ratio < 10), except BPS, which was outside the applicability domain of the

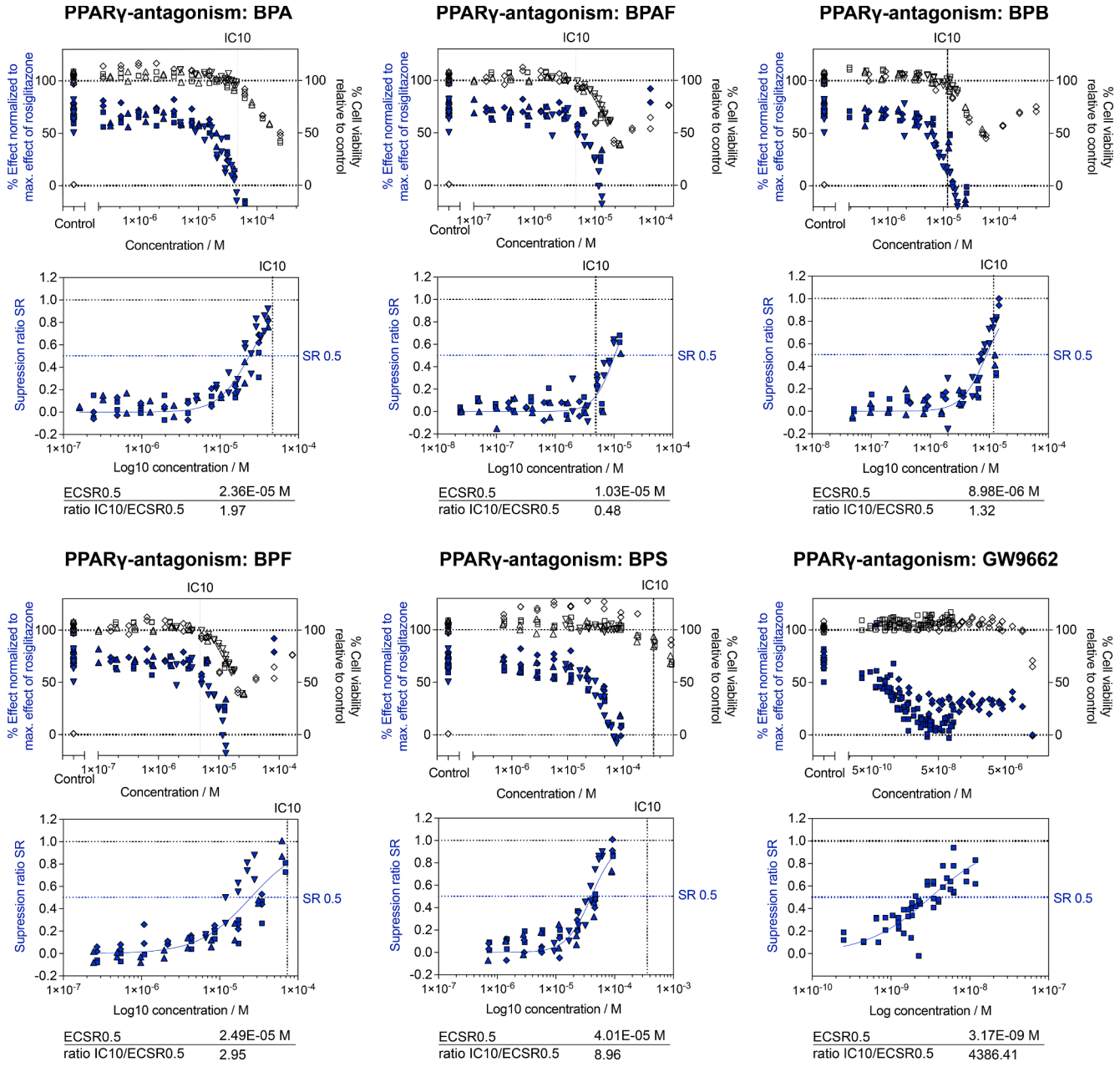

Fig. 2. Concentration-response curves of PPARγ-antagonism by bisphenols and the PPARγ inhibitor GW9662 in the PPARγ-UAS-bla 293H cell-based reporter gene assay. Inhibition of PPARγ activation, expressed as % of maximum effect that was induced by the positive control rosiglitazone starting at concentrations corresponding to EC_{80} of rosiglitazone (blue symbols, left y-axis) and cell viability relative to unexposed control cells (white symbols, right y-axis) are displayed against the analyte concentration range. Displayed for each analyte are the complete concentration–response curves. The vertical dotted line shows the 10% decrease in cell viability (IC_{10}) that was used as a concentration cut-off, below which the reporter gene activity was evaluated. Below them are the suppression ratios indicating the suppression of the maximum rosiglitazone effect against the Log10 compound concentration, the compound concentration at a suppression ratio (SR) of 0.5 (ECSR0.5), and the ratio of IC10/ECSR0.5. (For interpretation of the references to color in this figure legend, the reader is referred to the web version of this article.)

predictive model due to its high hydrophilicity (Table A.5). Activation of PPARγ was not detected under concentrations below the IC_{10} for bisphenol treatments (Supplementary data 7, Fig. A.3). Notably, BPB activated PPARγ only at concentrations above the IC_{10} (Supplementary data 7, Fig. A.3), which might be a result of the cytotoxicity burst (Escher et al. 2020). The PPARγ GeneBLAzer® cell line has a relatively high background signal of PPARγ activation, which might be due to fatty acid ligands present in the medium. Interestingly, this effect, which was set to 0%, was suppressed in a concentration-dependent fashion by BPA, BPB, BPF, and BPS (but not BPAF), indicating an antagonistic effect (Supplementary data 7, Fig. A.3). The antagonistic inhibition of PPARγ was confirmed by co-incubation of the compounds with rosiglitazone starting at EC_{80} (Fig. 2). According to the concentration at a 50% reduction of the activation induced by rosiglitazone ($EC_{SR0.5}$), the investigated compounds can be described by their antagonistic strength from low to high as BPS, BPF, BPA, BPB and GW9662 (Fig. 2). Notably, while GW9662 decreased rosiglitazone at low nM concentrations, the bisphenols revealed their antagonistic properties in a low to mid μM range. Additionally, BPAF exhibited an IC_{10} of 4.9 μM (Supplementary data 7, Table A.5), which was below the potential SR 0.5 (ratio $IC_{10}/EC_{SR0.5}$: 0.48) (Fig. 2), and thus did not allow conclusions on an antagonistic effect. For the other compounds, the $IC_{10}/EC_{SR0.5}$ ratio was above 1, indicating that the observed inhibition is not induced by a decrease in cell viability.

Thus, although SPR revealed that binding of the bisphenols to PPARγ is possible, the reporter gene assay results did not confirm a subsequent activation of PPARγ but rather suggested an antagonistic effect of the bisphenols.

3.2. SGBS cell viability

To analyze the biological effects induced by bisphenols in a cellular system, we used the human preadipocyte cell line SGBS. For determining the viability of SGBS cells under bisphenol exposure, the quantification of DAPI-stained DNA was performed. SGBS cells were differentiated for 12 days, with the addition of bisphenols in seven concentrations, ranging from 10 nM to 100 μM (Fig. 3 A, B). BPAF induced the highest decrease in cell viability, with an IC_{20} of 8.9 μM (Fig. 3 B). From low to high, the potential to decrease cell viability can be summerized as BPF < BPS < GW < BPA < BPB < BPAF. Similar results were observed using a lactate dehydrogenase (LDH) assay (Supplementary data 7, Fig. A.4). Due to the high toxicity of BPAF at 10 μM, results obtained with BPAF at this concentration need to be interpreted with caution.

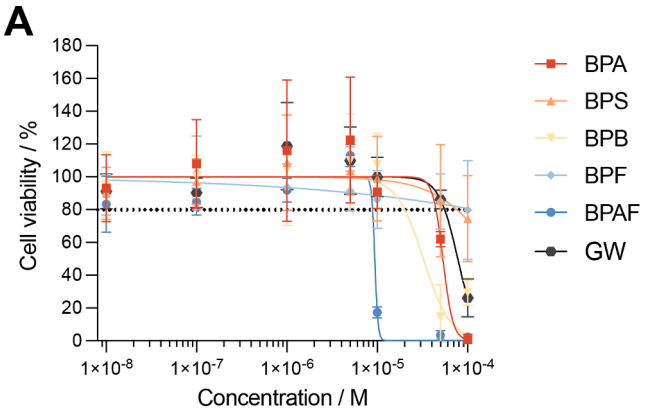

B

	BPF	BPS	GW	BPA	BPB	BPAF
IC_{20}	119.4 μM	76.0 μM	55.6 μM	44.3 μM	20.1 μM	8.9 μM

Fig. 3. Effect of bisphenols and GW9662 on the viability of SGBS cells. SGBS preadipocytes were differentiated using rosiglitazone for 12 days with the addition of bisphenols in concentrations ranging from 10 nM to 100 μM. Cell viability of a treatment was determined relative to the control, which was differentiated with rosiglitazone and 0.01% DMSO (A) Concentration-response curves of DAPI-stained cells on day 12. DAPI fluorescence ratios to the control are plotted in %. (B) Concentrations that induced 20% of cell viability reduction (IC_{20}), derived from the concentration–response curves.

3.3. Lipid quantification of bisphenol exposed SGBS cells

As for the determination of cell viabilities, biological effects of bisphenols on adipogenesis were assessed by exposure of SGBS preadipocytes to bisphenols for 12 days during differentiation with rosiglitazone (Fig. 4 A). The control was differentiated with rosiglitazone and contained 0.01% DMSO (Fig. 4 A). The PPARγ inhibitor GW9662 served as a reference for adipogenesis inhibition (Fig. 4 A). To determine the degree of adipocyte differentiation, lipid accumulation was visualized and quantified by Oil Red O staining as well as Nile Red staining normalized to DNA content staining with DAPI. SGBS preadipocytes were treated with 10 nM – 10 μM, of bisphenols since this concentration range did not substantially decrease cell viability, except 10 μM BPAF (Fig. 3). The amount of accumulated lipids was significantly lower at all concentrations tested for the different bisphenols and the well-established PPARγ-inhibitor GW9662 compared to the control using Oil Red O staining (Fig. 4 B, C). Similar results were observed using Nile Red staining normalized to the DNA content, although less significantly (Fig. 4 D). In contrast to GW9662, no pronounced concentration–response effect could be detected for any of the bisphenols (Fig. 4 C, D). Notably, the described low cell viability for 10 μM BPAF could be observed in the microscope image as well (Fig. 4 B) and is reflected by the substantial decrease of lipid accumulation (Fig. 4 C, D).

3.4. Proteomics

Next, we aimed to investigate the mode of action of the bisphenols during adipogenesis using global proteomics. To narrow down an appropriate time point at which SGBS cells could reach full differentiation, we first investigated a timeline of unexposed SGBS preadipocyte differentiation. SGBS preadipocytes were differentiated into adipocytes for 12 days, with samples taken at different time points (at 6 h and days 1, 2, 4, 8, and 12).

We reliably quantified 4465 proteins in at least three of five replicates. The number of significantly altered proteins (p.adj $\leq$ 0.05) steadily increased during the time course of differentiation (Fig. 5 A). Furthermore, a principal component analysis (PCA) indicated two separated groups: preadipocytes (day 0 to day 4) and differentiated adipocytes (day 8 and day 12) (Fig. 5 B). Ingenuity Pathway Analysis (IPA) revealed increased enrichment of pathways involved in lipid metabolism, energy production, and lipid storage during adipogenesis of SGBS cells (Fig. 5 C). Additionally, pathways assigned to immune or oxidative stress response and early protein synthesis were down-regulated in differentiated adipocytes. The changes were most substantial on day 12 of differentiation (Fig. 5 C). As a result, 12 days of differentiation were chosen as an appropriate time point to test the effect of BPA and its substitutes on adipogenesis.

Consequently, we treated SGBS cells for 12 days with BPA, BPAF, BPB, BPF, BPS, or PPARγ-antagonist GW9662. SGBS cells differentiated in the presence of the same amount of DMSO were used as an untreated control, and cells treated with GW9662 were used as a control for an adipogenesis-inhibiting effect mediated by PPARγ-inhibition (Fig. 4 A). FCs of protein abundances relative to the control were calculated, resulting in 3372 proteins, which were reliably quantified in three of four replicates. For the bisphenol treatments, 14% to 41% of the quantified proteins were significantly altered compared to the untreated control, except for 10 μM BPAF, which yielded 61% differentially abundant proteins, possibly due to its huge impact on cell viability at this concentration (Fig. 6 A). Treatment with GW9662 resulted in 35%

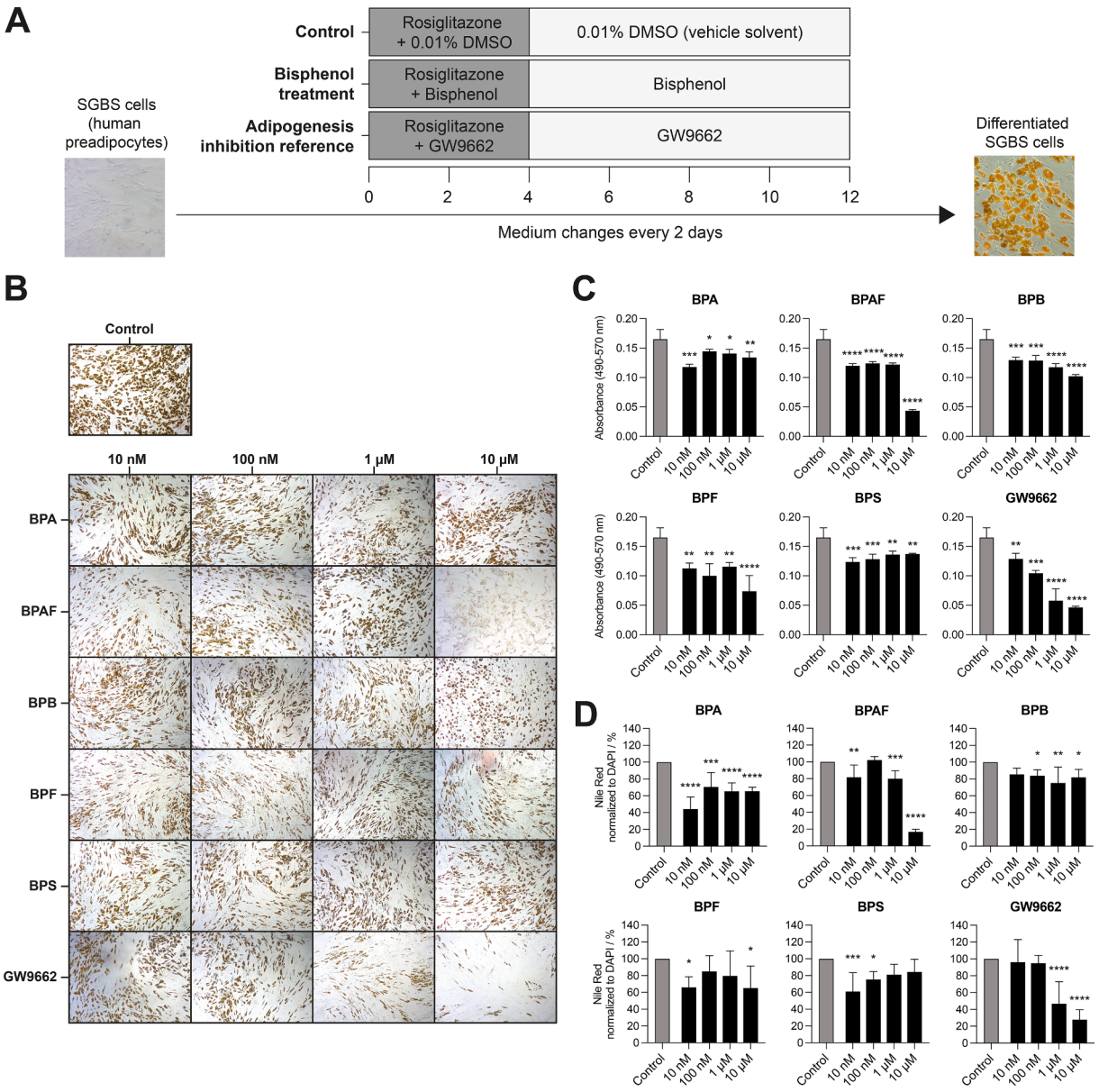

Fig. 4. Lipid accumulation of 12 days-differentiated SGBS cells under bisphenol treatments. (A) Overview of the experimental setup for the investigation of bisphenol effects on SGBS cell differentiation and, thus, adipogenesis. (B) Microscopy pictures of Oil Red O stained SGBS cells. Lipids were stained with Oil Red O and appear in red. (C) Quantification of Oil Red O stained lipids. (D) Quantification of Nile Red-stained lipids normalized to DAPI-stained DNA content (Fig. 3). Bar charts show mean ± SD. Statistically significant differences against the control are indicated by asterisks (* $p \leq 0.05$, ** $p \leq 0.01$, *** $p \leq 0.001$, **** $p \leq 0.0001$). (For interpretation of the references to color in this figure legend, the reader is referred to the web version of this article.)

to 57% altered proteins in a concentration-dependent way (Fig. 6 A).

Significantly enriched pathways were identified using Ingenuity Pathway Analysis (IPA) based on significantly ($p \leq 0.05$) affected proteins (Fig. 6 A). Pathways that were up-regulated in a time dependent manner during SGBS adipogenesis (Fig. 5 C) and other metabolism- and adipogenesis-related pathways were down-regulated by all bisphenol treatments (Fig. 6 B). This down-regulation appeared to be more prominent for BPF, BPB, and GW9662. Immune-related pathways such as *Chemokine Signaling*, *Role of PKR Interferon Induction and Antiviral Response*, and *IL-8 Signaling* were found to be up-regulated by the bisphenols as well as by GW9662. Additionally, pro-inflammatory pathways like *CXCR4 Signaling*, *NF-κB Activation by Viruses*, and *JAK/Stat Signaling* were activated by BPAF, BPB, BPF, and the two highest concentrations of BPA but were not augmented by GW9662 (Fig. 6 B). Interestingly, GW9662, BPAF, BPB, and BPF seemed to upregulate pathways involved in ECM remodeling and cytoskeleton signaling in contrast to BPA and BPS, which showed a down-regulation of those pathways for three of the four concentrations (Fig. 6 B). A complete heatmap of all significantly enriched pathways can be found in the supplementary information (Supplementary data 7, Fig. A.5).

Taken together, all studied bisphenols appeared to down-regulate metabolism-related pathways while up-regulating pro-inflammatory pathways similar to GW9662. These effects were observed starting at a compound concentration of 10 nM. BPA and BPS had a unique effect, with slightly less decreased metabolism-related pathways and a counter modulation of cytoskeleton-associated pathways compared to the other compounds.

Since our interaction studies revealed PPARγ-binding in an antagonistic manner, proteins induced by target genes of PPARγ which include common adipogenesis markers were investigated in more detail (Fig. 7) (Desvergne and Wahli 1999). GW9662 showed a substantial concentration-dependent decrease of PPARγ targets at the protein level

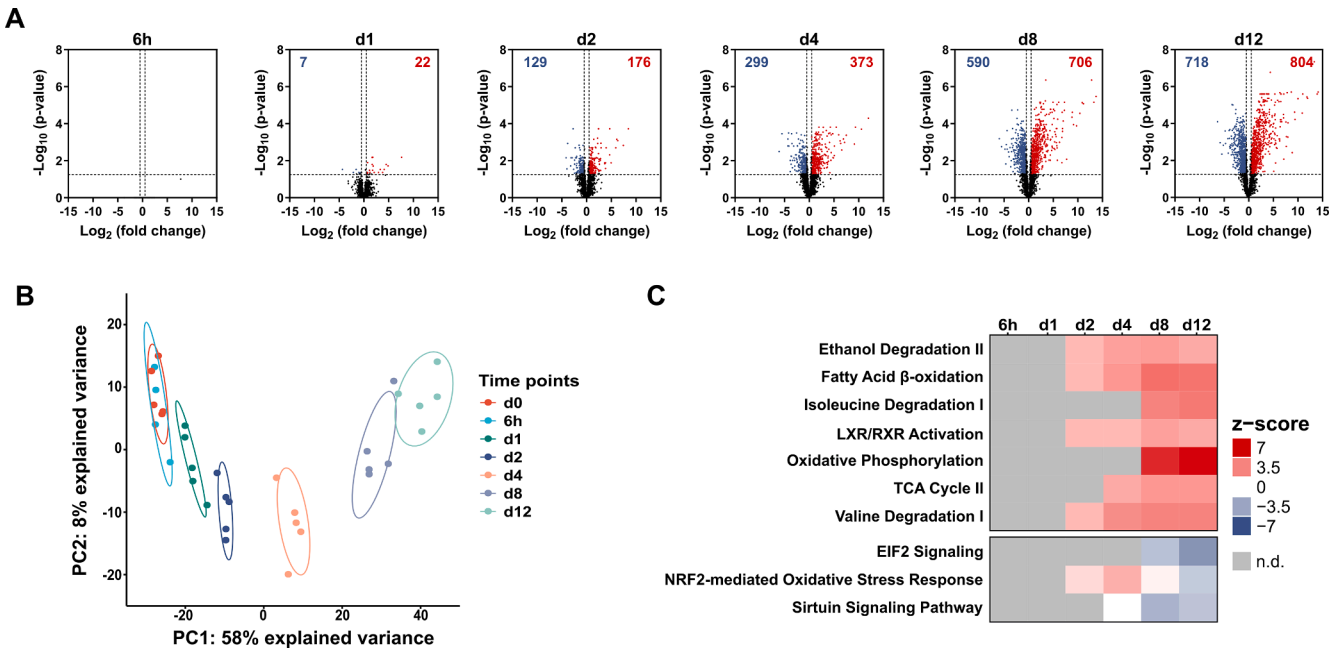

Fig. 5. Characterization of SGBS cell adipogenesis. (A) Volcano plots of differentially altered proteins for each time point (6 h, d1, d2, d4, d8, or d12 of differentiation). Highlighted proteins were significantly more (red, p.adj $\leq$ 0.05, Log_2(FC) $\geq$ 0.5) or less (blue, p.adj $\leq$ 0.05, Log_2(FC) $\geq$ -0.5) abundant than before differentiation (day 0). (B) Principal component analysis (PCA) of the obtained data of adipogenesis reveals a clear separation of each time point of differentiation. (C) Significantly enriched pathways were determined using Ingenuity Pathway Analysis (IPA) were determined using only significantly altered proteins (p.adj $\leq$ 0.05). The heatmap is colored based on z-scores calculated by IPA, indicating the direction of the pathway regulation (z-score > 0 pathway is up-regulated, z-score < 0 pathway is down-regulated). PRINT WITH COLOR. (For interpretation of the references to color in this figure legend, the reader is referred to the web version of this article.)

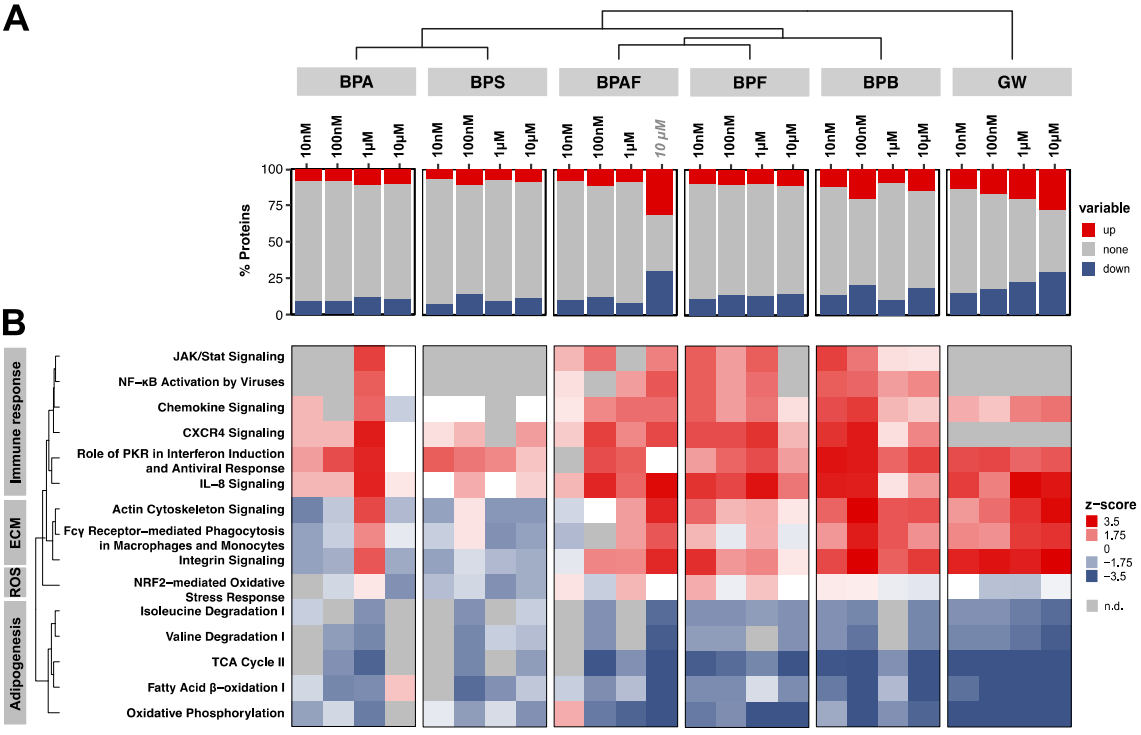

Fig. 6. General effects of treatment with bisphenols or PPARγ-antagonist GW9662 (GW) on the proteome of differentiating human adipocytes after 12 days of exposure. (A) Percentage of significantly ($p \leq 0.05$) altered proteins after exposure of SGBS cells compared to controls, which were subjected to Ingenuity Pathway Analysis (IPA). (B) Heatmap of selected significantly (p.adj $\leq$ 0.05) enriched pathways in treated SGBS cells. The 10 µM concentration of BPAF is marked in italic and grey because of its high decrease in cell viability at this concentration. The heatmap is colored based on z-scores calculated by IPA, indicating the direction of the pathway regulation (z-score > 0 pathway is up-regulated, z-score < 0 pathway is down-regulated, not detected is marked in grey).

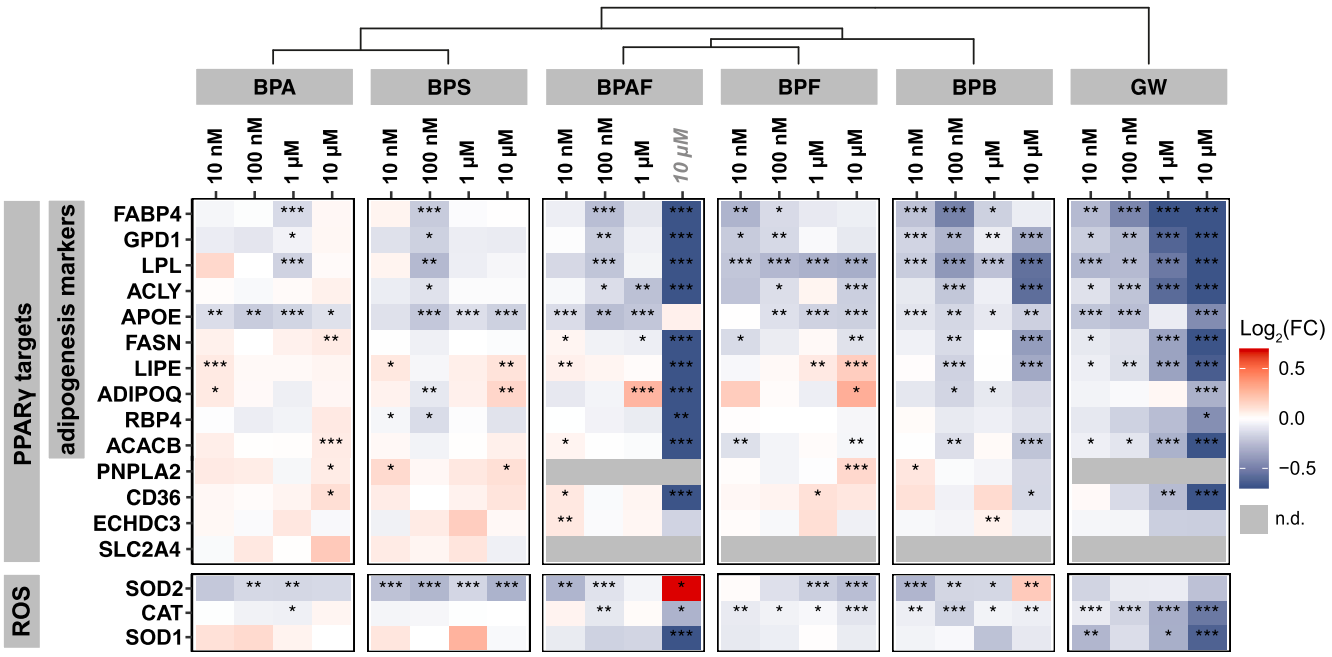

Fig. 7. Effect of bisphenols and PPARγ-inhibitor GW9662 (GW) on human adipocytes after 12 days of exposure during differentiation on the single protein level. Displayed proteins were obtained through proteomics analysis and are known target genes of PPARγ (top), which include common adipogenesis marker proteins, and ROS marker proteins (bottom). Changes are shown as the fold changes of Log_2(FC) treated SGBS cells compared to the control. The 10 µM concentration of BPAF is marked in italic and grey because of its high decrease in cell viability by>50%. Significant changes are labeled with asterisks (* $p \leq 0.05$, ** $p \leq 0.01$, *** $p \leq 0.001$).

compared to the unexposed control (Fig. 7). The bisphenols displayed a lesser but still decreased abundance of those proteins, with BPB showing the strongest effect, followed by BPF and BPAF (Fig. 7). PPARγ targets and adipogenesis markers fatty acid-binding protein 4 (FABP4), glycerol-3-phosphate dehydrogenase 1 (GPD1), lipoprotein lipase (LPL), and apolipoprotein E (APOE) were strongly down-regulated by GW9662, but also by BPB, BPF, BPAF starting at 10 nM, and, although lesser, by most concentrations of BPS and BPA (Fig. 7). Interestingly, some PPARγ targets like hormone-sensitive lipase (LIPE), Patatin-like phospholipase domain-containing protein 2 (PNPLA2), and CD36 were significantly increased upon treatment with BPA or BPS and to some extend also after exposure with BPB, BPF, and BPAF (Fig. 7). Adiponectin (ADIPOQ) appeared to be significantly decreased through GW9662 and BPB but partly increased by the other bisphenols (Fig. 7). Retinol binding protein 4 (RBP4) was overall barely changed by the bisphenols, but increased by GW9662. Nonetheless, intracellular adipokine levels of adiponectin and RBP4 do not necessarily allow conclusions about their release.

NRF2-mediated Oxidative Stress Response was slightly elevated at some concentrations of BPA, BPAF, BPB, and BPF (Fig. 6 B). The transcription factor Nuclear Factor Erythroid 2-related Factor 2 (NRF2) is activated in the first level of the oxidative stress response and regulates the expression of antioxidant genes including CAT, SOD1, and SOD2 (Vnukov et al. 2017). Taking a closer look at the protein level, catalase (CAT), superoxide dismutase 1 (SOD1), and superoxide dismutase 2 (SOD2) were mostly significantly decreased after bisphenol and GW9662 treatments (Fig. 7). The highest concentration of BPAF showed a notable decrease of PPARγ targets, CAT and SOD1, but highly increased SOD2 levels (Fig. 7). These changes, observed for 10 µM BPAF but not for the lower concentrations, can be attributed to its high toxicity (Fig. 3).

Overall, bisphenol and GW9662 treatments exhibited a decrease of PPARγ targets as well as ROS marker proteins.

3.5. Validation of proteomics results

Proteomic analysis revealed dysfunction of adipocytes upon bisphenol treatment, including potential PPARγ-inhibition and a pro-inflammatory state. These effects are, in general, associated with decreased insulin sensitivity (Dubuisson et al. 2011). Thus, insulin sensitivity was estimated using the relative expression ratio of pAKT/AKT after incubation with insulin. Insulin-responsive AKT signaling is a well-established marker for insulin sensitivity and is central to a functioning glucose uptake, which may result in insulin resistance when impaired (Manning and Toker 2017; Lo et al. 2013; Tindall et al. 2021). Decreased insulin sensitivity is indicated by a decreased ratio of pAKT/AKT after incubation with insulin. A concentration of 1 µM of BPA, BPB, BPS, and GW9662 exhibited significantly reduced ratios of pAKT/AKT upon insulin stimulation compared to the control (Fig. 8 A). 1 µM BPF provoked a decreased ratio, which was, however, not significant (Fig. 8 A). BPAF, on the other hand, exhibited significantly increased pAKT/AKT. Western blot images can be found in the supplement (Supplementary data 7, Fig. A.6). These data confirm an impaired insulin receptor signaling when adipocytes were exposed to BPA, BPB, BPF, or BPS.

Due to the altered adipokine level in the proteomics data, we evaluated the effects of the bisphenol treatments on the release of adipokines using 1 µM of compound. The signals of nine out of thirteen tested adipokines and cytokines were below the LegendPlex assay's detection limit. However, the quantification of adipokines and cytokines in the supernatant (Fig. 8 C) revealed significantly decreased adiponectin concentrations in all treatments except BPA, which was decreased only as a trend (Fig. 8 C). MCP1 concentrations were significantly increased in BPA, BPB, BPF, and GW9662 treatments, while BPS and BPAF showed at least a trend towards increased levels (Fig. 8 C). GW9662 displayed the most substantial differences in adipokine expression compared to the control (Fig. 8 C). RBP4 and adipsin were quantified but not significantly different from the control in bisphenol treatments (Fig. 8 C). Leptin, which was found to be below the limit of detection using the LegendPlex assay, was additionally assessed by ELISA at doses of 10 nM and 1 µM (Fig. 8 D). Significantly increased levels were detected for all treatments except BPB at 10 nM. 1 µM of BPB lead to a slight decrease in leptin, while 1 µM of BPF and GW9662 also increased leptin levels significantly (Fig. 8 D).

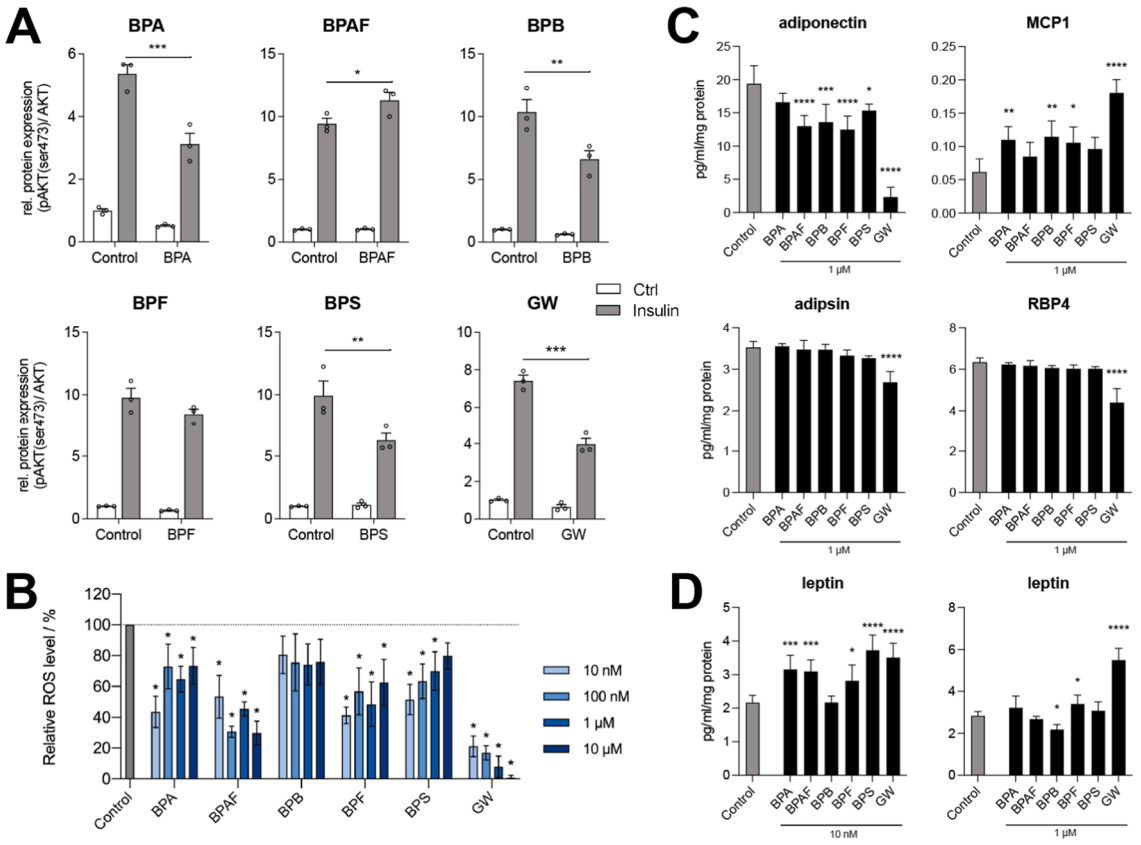

Fig. 8. Effects of bisphenol treatments on insulin signaling, as indicated by the ratio of pAKT/AKT, secreted adiponectin, and MCP1, as well as intracellular ROS levels. SGBS cells were exposed to bisphenols or GW9662 (GW) for 12 days during differentiation. (A) Relative pAKT(ser473)/AKT ratio of untreated cells (control) and cells treated with 1 µM of bisphenols or GW9662 determined by western blot analysis. Cells were incubated for 10 min with H_2O (Co) or 100 nM insulin (Insulin). Significant changes between control and treatment after insulin incubation were determined. (B) ROS levels were measured after SGBS cell incubation with 20 µM DCFDA for 45 min. (C) Concentrations of adipokines adiponectin, MCP1, adipsin, and RBP4 in SGBS cell supernatants after 12 days exposure with 1 µM bisphenols or GW9662 obtained via LegendPlex assay. (D) Leptin concentrations in SGBS cell supernatant after 12 days of exposure to 10 nM or 1 µM bisphenols or GW9662 obtained via ELISA. Significant changes are labeled with asterisks (* $p \leq 0.05$, ** $p \leq 0.01$, *** $p \leq 0.001$, **** $p \leq 0.0001$).

It was previously reported that BPA induces oxidative stress in various tissues and cell lines (Eid et al., 2015; Veiga-Lopez et al., 2015; Xin et al., 2014). However, the decrease of oxidative stress response-associated proteins (Fig. 7) does not suggest a similar effect in our experiments. To verify that the observed effects were not linked to elevated ROS levels, ROS were quantified on day 12 of differentiation. Thereby, BPA and its analogs did not increase cellular ROS levels after a chronic exposition compared with the control, reaching merely 80% of the control's ROS capacity (Fig. 8 C). Treatment with GW9662 resulted in the lowest ROS levels, with a concentration-dependent decrease of 30% – 1% (Fig. 8 C)), which reflects the observed down-regulation of metabolic processes (Fig. 6) since a main source of ROS is the oxidative phosphorylation (Li et al. 2013).

In summary, all treatments except BPAF turned the cells less sensitive to insulin. Adiponectin levels were significantly reduced in all treatments except BPA, and MCP1 was significantly increased in BPA, BPB, BPF, and GW9662 treatments, suggesting a pro-inflammatory effect and again, an impaired insulin sensitivity. ROS levels were decreased in response to bisphenol treatments compared to the control, thus contradicting the previously described induction of oxidative stress but being in line with the down-regulation of metabolic processes, which was observed based on the changes within the proteome (Fig. 6).

So far, the compounds (bisphenols or inhibitor) were applied during the 12 days of differentiation to unravel their effects on adipogenesis. To investigate the effects bisphenols have on mature adipocytes, 12 days differentiated adipocytes were exposed to 1 µM of bisphenol or GW9662 for 3 days after differentiation, and their effects on cell viability, insulin sensitivity, and adipokine release were determined (Supplementary data 7, Fig. A.7). BPA, BPS, and BPAF revealed reduced pAKT/AKT, indicating impairment of insulin signaling (Supplementary data 7, Figs. A.7 and A.8). Nonetheless, the compounds had no effect on adipogenesis or cell viability, even after 8 days of exposure (Supplementary data 7, Fig. A.7). Of the assessed adipokines, i.e. leptin, adipsin, and MCP1, only MCP1 showed an increase upon GW9662 exposure and a decrease through BPA and BPS (Supplementary data 7, Fig. A.7). This suggests that bisphenols also impair insulin sensitivity when exposed to differentiated adipocytes, highlighting the potential of not only BPA, but also its substitutes to affect human health.

4. Discussion

BPA, a commonly used plastic additive with previously reported obesogenic properties, is increasingly substituted by analogs, creating the necessity to evaluate their obesogenic properties compared to BPA (Ji and Choi 2013). Although miscellaneous effects of BPA on adipocyte function were described, the majority of studies observed an adipogenesis-promoting effect (Ohlstein et al. 2014; Masuno et al. 2005; Helies-Toussaint et al. 2014; Martinez et al. 2020). Moreover, some studies point to similar obesogenic properties for BPA alternatives: Masuno et al. (2005) analyzed metabolic disruptive effects of BPA-related chemicals in murine preadipocytes and found eight analogs to increase adipocyte differentiation and triglyceride accumulation comparable to BPA's effect. Others confirmed adipogenesis induction through BPS in human adipocytes (Boucher, Ahmed, and Atlas 2016)

and accelerated fat deposition in zebrafish *in vivo* (Wang et al. 2018). More recently, Martinez et al. (2020) reported higher obesogenic properties for BPS and BPF compared to BPA, including increased lipid production and differentiation of murine adipocytes, as well as an increase of PPARγ and FABP4 expression by BPS. Although they confirmed sufficient cell viability, environmentally relevant concentrations, which were in median 6.50 ng/ml (28.5 nM) in the serum of 97.5% of participants in a recent study (Yang et al. 2020), are 1000-fold lower than the used concentration of 32 μM.

PPARγ, which plays a pivotal role in regulating adipogenesis and lipid metabolism (Lefterova et al. 2014; Tontonoz et al. 1994), is a relevant target for the obesogenic disruption caused by various environmental contaminants (Masuno et al. 2005). The activation of PPARγ was previously reported as a possible cause for the adipogenesis-promoting effects of BPA (Ahmed and Atlas 2016). To test this hypothesis for distinct BPA analogs, their molecular interactions with PPARγ were investigated in the present study. While we could confirm the binding of BPA to PPARγ, BPB exhibited an even higher binding affinity, and the other analogs showed a significant binding signal as well. Interestingly, binding of the PPARγ-antagonist GW9662 was demonstrated via SPR before (Yu et al. 2004).

Contrary to expectations, the reporter gene assay revealed a concentration-dependent decrease of the background signal indicating an antagonistic effect on PPARγ. By the parallel application of the agonist rosiglitazone and the bisphenols antagonistic properties were revealed for all bisphenols except BPAF at low to mid μM concentrations that did not decrease cell viability. Previously, PPARγ activation through BPA was observed in a mid to high μM concentration range (Ahmed and Atlas 2016). However, such concentrations were reported to induce cytotoxic effects (Ohlstein et al. 2014), being in line with our SGBS cell viability assays and the IC_{10} values obtained in the reporter gene assay PPARγ-UAS-bla. Thus, PPARγ activation in other studies may be affected by a cell viability decrease resulting from the applied compound concentrations (Escher et al. 2020), similar to what we observed at high concentrations of BPB. In accordance with that, Chamorro-García et al. (2012) did not observe any activation of PPARγ through BPA in their transient transfection assays using a lower concentration range as well. Contrary to our results, they did not observe a PPARγ-antagonism, which may be due to the difference in cell line or their high background concentrations of the agonist rosiglitazone (Chamorro-García et al. 2012; Neale and Leusch 2015).

Notably, the LDH assay was highly affected by the different differentiation levels and, thus, metabolic rates of the adipocytes, which required normalization to the lowest compound concentration (10 nM). This limitation was not shared by the method of cell viability determination via quantitative DAPI staining of the DNA content, making it more reliable for cell viability assessment in adipocytes. Additionally, coupled with simultaneous Nile Red staining of lipids, we agree with Aldridge et al. (2013) that this method allows for a less subjective quantification of lipid accumulation compared to Oil Red O staining alone.

The observed binding to PPARγ and the concentration-dependent inhibition of the receptor emphasize an antagonistic effect, which was, to our knowledge, not described for BPA and its analogs before in this detail. Importantly, PPARγ-inhibition contradicts adipogenesis-promoting effects of BPA and its analogs and instead suggests an inhibiting effect on adipogenesis. This adipogenesis inhibition is supported by our results, which show a decrease in lipid accumulation, adipogenesis, metabolism-related pathways, and adipogenesis markers like FABP4, LPL, and APOE (Moseti, Regassa, and Kim 2016) on the proteome level for all tested bisphenols, starting at 10 nM. Furthermore, these findings are in good agreement with De Filippis, Li, and Rosen (2018), who exposed human and mouse adipocytes to BPA over 7 days, with cell culture medium changes every 2 days, and did not observe changes in lipid accumulation and mRNA levels of adipogenesis markers at low concentrations (1–10 nM), but a decrease of those at 100 nM.

Overall, bisphenol-treated cells exhibited decreased adipogenesis similar to the PPARγ-antagonist GW9662 here, although to a lesser extent, indicating that they may act through similar mechanisms. Important adipogenesis marker and direct PPARγ targets include FABP4, GPD1, LPL, ACYL, and APOE (Nakachi et al. 2008; Sledzinski et al. 2013; Akiyama et al. 2002), which are strongly down-regulated by GW9662, but also by BPB, BPF, BPAF, and most concentrations of BPS and BPA. From this data, we conclude that PPARγ inhibition is at least one of the central adverse effects caused by BPA and its substitutes in human adipocytes. Interestingly, a few PPARγ targets appear to be unchanged or increased in certain concentrations, particularly for BPA and BPS, suggesting more complex mechanisms. Thus, ligand-specific cofactors of the PPARγ-complex and DNA response elements may be investigated further to fully understand these results. Additionally, investigation of BPA and BPS interaction with further interaction partners in the cell may be of interest. Moreover, only GW9662 presented concentration-dependent effects, which can be explained by the fact that endocrine disruptors, and in particular BPA, are known to have non-monotonic response curves (Vandenberg 2014).

Interestingly, while PPARγ-antagonism was only detected at μM-concentrations, a decrease of direct PPARγ targets was shown at the lowest tested concentration of 10 nM via proteomic analysis for all BPB, BPF, and BPAF. These results indicate that an inhibitory effect may be reached by environmentally relevant concentrations if the cells are continuously exposed to the bisphenols over a longer time span.

A discrepancy between the adipogenesis-promoting effects of other studies and the adipogenesis-inhibiting effects of our findings can likely be explained by the differences in the experimental setup and tested cell strain. Other authors have used a one-time exposure at the beginning of differentiation, as well as concentrations in a μM range, while we used a more physiologic set up with chronic exposure in a nM to low μM range (Martinez et al. 2020; Ohlstein et al. 2014; Masuno et al. 2005; Helies-Toussaint et al. 2014). After reviewing a variety of studies, Legeay and Faure concluded that BPA induces adipocyte differentiation in a μM concentration range and adipocyte dysfunction, including a pro-inflammatory effect with a subsequent decrease in insulin sensitivity in a nM concentration range (Legeay and Faure 2017). In our opinion, it is essential to test continuous long-term exposures and include nM concentrations, which represent physiological conditions more closely (Yang et al. 2020). Nonetheless, the influence of a species- and cell strain-specific effect cannot be ruled out, as demonstrated by Chamorro-García et al. (2012), who reported that while BPA promoted adipogenesis in murine adipocytes, it failed to induce this process in human mesenchymal stem cells at low concentrations of 1 nM – 1 μM. Since SGBS cells were extracted from the subcutaneous adipose tissue of an infant (Wabitsch et al. 2001), and different adipose tissue depots were shown to have different functionalities (Iacobini et al. 2019; Zwick et al. 2018; Tchkonia et al. 2002), our findings might give information on how this kind of tissue responds to bisphenol exposure.

BPA has been reported to induce pro-inflammatory effects, such as the release of the pro-inflammatory factors interleukin 6 (IL-6) and interferon γ (IFN-γ) together with the activation of JNK/Stat3/NFκ-B pathways (Valentino et al. 2013; Ariemma et al. 2016). Consistent with that, immune-related pathways were up-regulated in the here investigated bisphenol treatments, including *JAK/Stat Signaling*, *NFκ-B Activation by Viruses*, and *Role of PKR Interferon Induction and Antiviral Response*. The bisphenols exhibited more substantial pro-inflammatory effects than GW9662, which is known to increase inflammation by blocking the anti-inflammatory properties of PPARγ (Dubuisson et al. 2011). This may indicate the pro-inflammatory state being a consequence of PPARγ-inhibition by the bisphenols, which might be even intensified via PPARγ-independent mechanisms.

Another consequence of PPARγ-inhibition is decreased insulin sensitivity, which is reflected by a reduced ratio of pAKT/AKT through GW9662 compared to the control (Dubuisson et al. 2011). BPA, BPB, BPS, and, to a lesser extent, BPF showed the same reduced insulin

signaling. Exposure of mature SGBS adipocytes to BPA, BPS, and BPAF also resulted in a decrease of pAKT, suggesting a similar reducing effect on insulin sensitivity even in already differentiated adipocytes. Previous studies have also reported the suppression of insulin signaling and subsequent reduction of glucose uptake through BPA (Valentino et al. 2013; Alonso-Magdalena et al. 2010). Recently, Martinez et al. (2020) investigated pAKT/AKT after BPA, BPS, and BPF treatment but did not observe significant changes. Unlike our study, they used a one-time exposure at the beginning of differentiation, which suggests the necessity of a physiologically relevant, continuous, long-term exposure (Martinez et al. 2020).

Thus, we suggest that BPA and some of its analogs decrease insulin sensitivity in human adipocytes, possibly mediated by PPARγ-inhibition. This may similarly affect other tissues than the adipose tissue since PPARγ can be found in various cell types. Other cell types, as well as *in vivo* effects, need to be investigated further. Suppressed insulin signaling may further increase the inflammatory state through abolished insulin-mediated inhibition of Nfκ-B and Egr-1 expression (Sun, Li, and Gao 2014). Impaired insulin signaling could be a supporting factor for the observed bisphenol-induced pro-inflammatory effects.

Moreover, altered secretion of adipokines is linked to insulin resistance (Ziemke and Mantzoros 2010). In particular, adiponectin, a known PPARγ target gene, has anti-inflammatory and anti-diabetic properties (Cnop et al. 2003; Straub and Scherer 2019). Therefore, it was described to be less abundant in patients with obesity and co-morbidities, such as type 2 diabetes and cardiovascular diseases (Ziemke and Mantzoros 2010). Adiponectin was found to be decreased by bisphenol treatments, as confirmed by proteomics and quantification in cell culture supernatants. Additionally, adiponectin was reported to enhance adipocyte differentiation (Fu et al. 2005). Thus, reduced adiponectin may affect adipogenesis, as observed in bisphenol treatments. Hugo et al. (2008) have described a significant decrease of adiponectin release in human adipocytes under environmentally relevant BPA concentrations, which was not estrogen receptor-mediated, suggesting the involvement of other nuclear receptors. We propose here a PPARγ inhibition-mediated suppression of adiponectin release by BPA and its analogs. Nonetheless, we cannot exclude the interference of other nuclear receptors, which have not been investigated in this study.

Another adipokine connected to the pathogenesis of obesity and related diseases is the pro-inflammatory adipokine MCP1, also known as CC-chemokine ligand 2 (CCL2) (Sell and Eckel 2007). It mediates macrophage infiltration into the adipose tissue, leading to chronic inflammation and promoting systemic insulin resistance (Sartipy and Loskutoff 2003). Thus, MCP1 increase in the SGBS supernatant after bisphenol treatment may accelerate an inflammatory state of adipose tissue. MCP1 expression is insulin-responsive; therefore, the observed MCP1 increase in the SGBS supernatant after bisphenol treatment may be connected to impaired insulin signaling (Sartipy and Loskutoff 2003). GW9662 shows the most significant effect on adiponectin and MCP1 release, which can be attributed to the antagonistic effect towards PPARγ.

Moreover, it was previously reported that leptin blood levels positively correlate with insulin resistance independently of an obesity phenotype (Zuo et al. 2013). Leptin modulates adipocyte metabolism by inhibiting lipid accumulation and reducing insulin sensitivity (Harris 2014). This suggests that the detected elevation of leptin levels in bisphenol-treated adipocytes during differentiation may be linked to the overserved reduction of insulin sensitivity, potentially contributing to insulin resistance in adipose tissue.

Other studies have repeatedly shown that BPA induces oxidative stress in different tissues, and Song et al. (2014) proposed a link between BPA-induced insulin resistance and oxidative stress in rats (Eid, Eissa, and El-Ghor 2015; Xin et al. 2014; Veiga-Lopez et al. 2015). To investigate this connection in our human cell system, oxidative stress-associated proteins of the assessed proteome were considered, and relative ROS levels of bisphenol treatments were compared. Oxidative stress response-associated proteins CAT, SOD1, and SOD2 were overall decreased in bisphenol and GW9662 treatments compared to the control, except 10 μM BPAF and 10 μM BPB. BPAF and BPB showed the highest toxicity among the BPA analogs, explaining the divergent increase in SOD2 abundance as a response to apoptotic stress. To verify that bisphenols do not induce oxidative stress in SGBS cells, intracellular ROS levels were quantified on day 12 of treatment. Consistent with the changes on the protein level, ROS appeared to be decreased upon bisphenol and GW9662 treatments compared to the control, presumably caused by the varying differentiation level and being in line with decreased metabolic processes. Thus, oxidative stress is most certainly not the explanation for the observed adipogenesis-inhibiting effects of BPA and its analogs.

In summary, our findings indicate that BPA and its substitutes inhibited adipogenesis of human preadipocytes, induced an inflammatory-like state in adipocytes and impaired insulin signaling, as well as adipokine secretion (Fig. 9). At least to some degree, these effects may be mediated by PPARγ inhibition and occurred at environmentally relevant concentrations of 10 nM.

Notably, the adipose tissue of obese and overweight individuals was reported to have decreased expression of adipogenesis markers, such as FABP4 and adiponectin, impaired insulin signaling, and increased expression of ECM remodeling (Matulewicz et al. 2017; Yang et al. 2004). These reports are in line with our findings and suggest that BPA and its substitutes may prevent a healthy expansion of the subcutaneous adipose tissue, which is, next to the visceral adipose tissue, the most important storage site for excess calories (Longo et al. 2019). By inhibiting the differentiation of preadipocytes, BPA and its substitutes may promote a hypertrophic expansion of the adipose tissue, resulting in chronic inflammation, insulin resistance, and adipocyte dysfunction (Longo et al. 2019).

Hammarstedt et al. (2018) describe that a limited expansion and storage capacity of the subcutaneous adipose tissue resulting from hypertrophy is strongly associated with obesity-associated metabolic complications. Besides its relevance in obese individuals, a hypertrophic adipose tissue can also cause type 2 diabetes in lean subjects (Acosta et al. 2016; Henninger et al. 2014).

5. Conclusion

BPA and its substitutes BPAF, BPB, BPF, and BPS inhibited adipogenesis of human preadipocytes, promoted an inflammatory state, led to dysregulation of adiponectin and MCP1 release, and decreased insulin sensitivity. Thus, the investigated substitutes have at least similar metabolic disruptive properties as BPA and may promote a hypertrophic dysfunction of adipose tissue. This effect, in turn, may contribute to a persistently increased risk of developing the metabolic syndrome. The fact that these effects were observed in a human cell culture system and under a physiologically relevant chronic exposure, including environmentally realistic concentrations, renders these findings highly relevant for a reasonable obesogenic evaluation of BPA and its substitute compounds. Therefore, we urge colleagues to study the substitutes' effects in relevant *in vitro*, *ex vivo*, and *in vivo* systems and regulatory entities not to classify them as safe alternatives.

Funding

This work was supported by the German Federal Environmental Foundation (DBU) under a personal fellowship of Alexandra Schaffert. Martin von Bergen and Kristin Schubert are grateful for support by the Helmholtz-Centre for Environmental Research (UFZ)-funded platform *ProMetheus* for proteome and metabolome analysis. Laura Krieg, Martin von Bergen, Matthias Blüher, Kathrin Landgraf, Antje Körner, and John T. Heiker are thankful for funding by the German Research Council (DFG) for the Clinical Research Center "Obesity Mechanisms" SFB 1052/2 (B1, C5, C7, Z3).

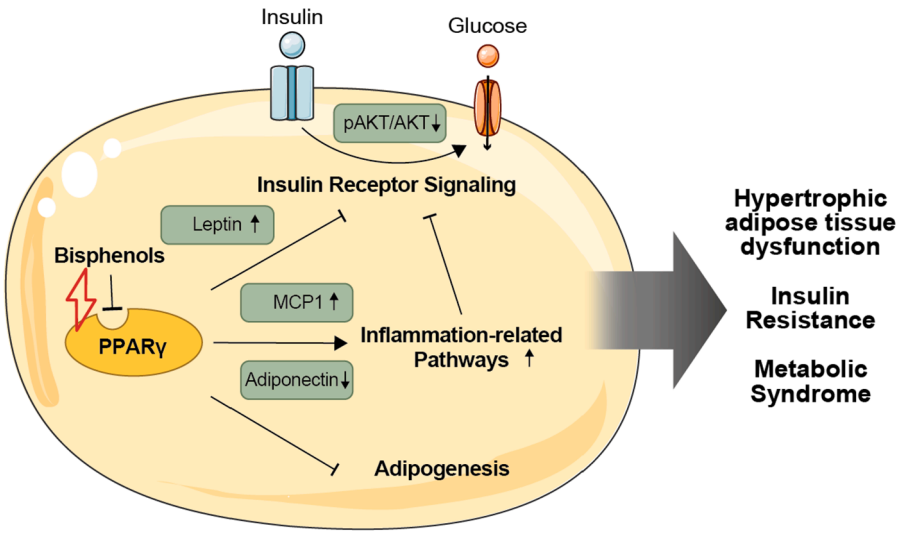

Fig. 9. Proposed bisphenol mode of action in SGBS cells. Through their antagonistic effect on PPARγ, BPA and its substitutes led to decreased adipogenesis and adiponectin levels, as well as increased MCP1 and leptin release. Consequently, adipocytes entered a chronic inflammation-like state and subsequently reduced insulin signaling. Ultimately, these dysfunctions could promote hypertrophy of adipocytes, leading to insulin resistance and development of the metabolic syndrome.

CRediT authorship contribution statement

Alexandra Schaffert: Conceptualization, Methodology, Investigation, Validation, Writing - original draft, Visualization. **Laura Krieg:** Conceptualization, Methodology, Investigation, Writing - original draft, Visualization. **Juliane Weiner:** Validation, Visualization, Writing - review & editing. **Rita Schlichting:** Methodology, Investigation, Visualization, Writing - review & editing. **Elke Ueberham:** Resources, Supervision, Writing - review & editing. **Isabel Karkossa:** Data curation, Supervision, Writing - review & editing. **Mario Bauer:** Validation. **Kathrin Landgraf:** Supervision, Writing - review & editing. **Kristin M. Junge:** Validation, Writing - review & editing. **Martin Wabitsch:** Resources, Writing - review & editing. **Jörg Lehmann:** Resources, Writing - review & editing. **Beate I. Escher:** Resources, Project administration, Writing - review & editing. **Ana C. Zenclussen:** Resources, Project administration, Writing - review & editing. **Antje Körner:** Resources, Project administration, Writing - review & editing. **Matthias Blüher:** Writing - review & editing. **John T. Heiker:** Writing - review & editing. **Martin Bergen:** Supervision, Writing - review & editing, Project administration. **Kristin Schubert:** Conceptualization, Supervision, Writing - review & editing, Project administration.

Declaration of Competing Interest

The authors declare that they have no known competing financial interests or personal relationships that could have appeared to influence the work reported in this paper.

Appendix A. Supplementary material

Supplementary data to this article can be found online at https://doi.org/10.1016/j.envint.2021.106730.

References

Acconcia, F., Pallottini, V., Marino, M., 2015. Molecular Mechanisms of Action of BPA. Dose-response: a publication of International Hormesis Society, 13: 1559325815610582-82.
Acosta, J.R., Douagi, I., Andersson, D.P., Backdahl, J., Ryden, M., Arner, P., Laurencikiene, J., 2016. Increased fat cell size: a major phenotype of subcutaneous white adipose tissue in non-obese individuals with type 2 diabetes. Diabetologia 59, 560–570.
Adrian, A.D., Cole, A., 2018. xlsx: Read, Write, Format Excel 2007 and Excel 97/2000/XP/2003 Files. R package version (6), 1.
Ahmed, S., Atlas, E., 2016. Bisphenol S- and bisphenol A-induced adipogenesis of murine preadipocytes occurs through direct peroxisome proliferator-activated receptor gamma activation. Int. J. Obes. (Lond) 40, 1566–1573.
Akiyama, T.E., Sakai, S., Lambert, G., Nicol, C.J., Matsusue, K., Pimprale, S., Lee, Y.H., Ricote, M., Glass, C.K., Brewer Jr., H.B., Gonzalez, F.J., 2002. Conditional disruption of the peroxisome proliferator-activated receptor gamma gene in mice results in lowered expression of ABCA1, ABCG1, and apoE in macrophages and reduced cholesterol efflux. Mol. Cell Biol. 22, 2607–2619.
Aldridge, A., Kouroupis, D., Churchman, S., English, A., Ingham, E., Jones, E., 2013. Assay validation for the assessment of adipogenesis of multipotential stromal cells–a direct comparison of four different methods. Cytotherapy 15, 89–101.
Alonso-Magdalena, P., Vieira, E., Soriano, S., Menes, L., Burks, D., Quesada, I., Nadal, A., 2010. Bisphenol A exposure during pregnancy disrupts glucose homeostasis in mothers and adult male offspring. Environ. Health Perspect. 118, 1243–1250.
Ananda, M., 2019. splitstackshape: stack and reshape datasets after splitting concatenated values. R Package Version 1 (4), 8.
Andrej-Nikolai, S., 2018. qpcR: modelling and analysis of real-time PCR data. R Package Version 1.4-1.
ANSES, 2014. 'Annex XV Restriction Report Proposal For a Restriction; BPA'.
Ariemma, F., D'Esposito, V., Liguoro, D., Oriente, F., Cabaro, S., Liotti, A., Cimmino, I., Longo, M., Beguinot, F., Formisano, P., Valentino, R., 2016. Low-dose bisphenol-a impairs adipogenesis and generates dysfunctional 3T3-L1 adipocytes. PLoS ONE 11, e0150762.
Bannuscher, A., Karkossa, I., Buhs, S., Nollau, P., Kettler, K., Balas, M., Dinischiotu, A., Hellack, B., Wiemann, M., Luch, A., von Bergen, M., Haase, A., Schubert, K., 2020. A multi-omics approach reveals mechanisms of nanomaterial toxicity and structure-activity relationships in alveolar macrophages. Nanotoxicology 14, 181–195.
Boucher, J.G., Ahmed, S., Atlas, E., 2016. Bisphenol S induces adipogenesis in primary human preadipocytes from female donors. Endocrinology 157, 1397–1407.
Chamorro-García, R., Kirchner, S., Li, X., Janesick, A., Casey, S.C., Chow, C., Blumberg, B., 2012. Bisphenol A diglycidyl ether induces adipogenic differentiation of multipotent stromal stem cells through a peroxisome proliferator-activated receptor gamma-independent mechanism. Environ. Health Perspect. 120, 984–989.
Cnop, M., Havel, P.J., Utzschneider, K.M., Carr, D.B., Sinha, M.K., Boyko, E.J., Retzlaff, B.M., Knopp, R.H., Brunzell, J.D., Kahn, S.E., 2003. Relationship of adiponectin to body fat distribution, insulin sensitivity and plasma lipoproteins: evidence for independent roles of age and sex. Diabetologia 46, 459–469.
Darbre, P.D., 2017. Endocrine disruptors and obesity. Curr. Obes Rep. 6, 18–27.
De Filippis, E., Li, T., Rosen, E.D., 2018. Exposure of adipocytes to bisphenol-A in vitro interferes with insulin action without enhancing adipogenesis. PLoS ONE 13, e0201122.
Desvergne, B., Wahli, W., 1999. Peroxisome proliferator-activated receptors: nuclear control of metabolism*. Endocr. Rev. 20, 649–688.
Ding, S., Fan, Y., Zhao, N., Yang, H., Ye, X., He, D., Jin, X., Liu, J., Tian, C., Li, H., Xu, S., Ying, C., 2014. High-fat diet aggravates glucose homeostasis disorder caused by chronic exposure to bisphenol A. J. Endocrinol. 221, 167–179.
Dubuisson, O., Dhurandhar, E.J., Krishnapuram, R., Kirk-Ballard, H., Gupta, A.K., Hegde, V., Floyd, E., Gimble, J.M., Dhurandhar, N.V., 2011. PPARgamma-independent increase in glucose uptake and adiponectin abundance in fat cells. Endocrinology 152, 3648–3660.
ECHA, European Chemicals Agency. https://echa.europa.eu/hot-topics/bisphenol-a.
Eid, Jehane I., Eissa, Shaymaa M., El-Ghor, Akmal A., 2015. Bisphenol A induces oxidative stress and DNA damage in hepatic tissue of female rat offspring. J. Basic Appl. Zool. 71, 10–19.

Escher, B. I., M. Allinson, R. Altenburger, P. A. Bain, P. Balaguer, W. Busch, J. Crago, N. D. Denslow, E. Dopp, K. Hilscherova, A. R. Humpage, A. Kumar, M. Grimaldi, B. S. Jayasinghe, B. Jarosova, A. Jia, S. Makarov, K. A. Maruya, A. Medvedev, A. C. Mehinto, J. E. Mendez, A. Poulsen, E. Prochazka, J. Richard, A. Schifferli, D. Schlenk, S. Scholz, F. Shiraishi, S. Snyder, G. Su, J. Y. M. Tang, B. Burg, S. C. v. d. Linden, I. Werner, S. D. Westerheide, C. K. C. Wong, M. Yang, B. H. Y. Yeung, X. Zhang, and F. D. L. Leusch. 2014. 'Benchmarking Organic Micropollutants in Wastewater, Recycled Water and Drinking Water with In Vitro Bioassays', Environmental Science & Technology, 48: 1940-56.

Escher, B.I., Glauch, L., König, M., Mayer, P., Schlichting, R., 2019. Baseline toxicity and volatility cutoff in reporter gene assays used for high-throughput screening. Chem Res Toxicol 32, 1646–1655.

Escher, B.I., Henneberger, L., Konig, M., Schlichting, R., Fischer, F.C., 2020. Cytotoxicity burst? Differentiating specific from nonspecific effects in Tox21 in vitro reporter gene assays. Environ. Health Perspect. 128, 77007.

Fu, Y., Luo, N., Klein, R.L., Garvey, W.T., 2005. Adiponectin promotes adipocyte differentiation, insulin sensitivity, and lipid accumulation. J. Lipid Res. 46, 1369–1379.

Gu, Z., Gu, L., Eils, R., Schlesner, M., Brors, B., 2014. circlize Implements and enhances circular visualization in R. Bioinformatics 30, 2811–2812.

Hammarstedt, A., Gogg, S., Hedjazifar, S., Nerstedt, A., Smith, U., 2018. Impaired adipogenesis and dysfunctional adipose tissue in human hypertrophic obesity. Physiol. Rev. 98, 1911–1941.

Harris, R.B., 2014. Direct and indirect effects of leptin on adipocyte metabolism. Biochim. Biophys. Acta 1842, 414–423.

Helies-Toussaint, C., Peyre, L., Costanzo, C., Chagnon, M.C., Rahmani, R., 2014. 'Is bisphenol S a safe substitute for bisphenol A in terms of metabolic function? An in vitro study'. Toxicol Appl Pharmacol 280, 224–235.

Henninger, A.M., Eliasson, B., Jenndahl, L.E., Hammarstedt, A., 2014. Adipocyte hypertrophy, inflammation and fibrosis characterize subcutaneous adipose tissue of healthy, non-obese subjects predisposed to type 2 diabetes. PLoS ONE 9, e105262.

Hughes, C.S., Foehr, S., Garfield, D.A., Furlong, E.E., Steinmetz, L.M., Krijgsveld, J., 2014. Ultrasensitive proteome analysis using paramagnetic bead technology. Mol. Syst. Biol. 10, 757.

Hughes, C.S., Moggridge, S., Müller, T., Sorensen, P.H., Morin, G.B., Krijgsveld, J., 2019. Single-pot, solid-phase-enhanced sample preparation for proteomics experiments. Nat. Protoc. 14, 68–85.

Hugo, E.R., Brandebourg, T.D., Woo, J.G., Loftus, J., Alexander, J.W., Ben-Jonathan, N., 2008. Bisphenol A at environmentally relevant doses inhibits adiponectin release from human adipose tissue explants and adipocytes. Environ. Health Perspect. 116, 1642–1647.

Iacobini, C., Pugliese, G., Blasetti Fantauzzi, C., Federici, M., Menini, S., 2019. Metabolically healthy versus metabolically unhealthy obesity. Metabolism 92, 51–60.

Ivry Del Moral, L., Le Corre, L., Poirier, H., Niot, I., Truntzer, T., Merlin, J.F., Rouimi, P., Besnard, P., Rahmani, R., Chagnon, M.C., 2016. Obesogen effects after perinatal exposure of 4,4'-sulfonyldiphenol (Bisphenol S) in C57BL/6 mice. Toxicology 357–358, 11–20.

Jan, G., 2019. calibrate: Calibration of Scatterplot and Biplot Axes. R package version 1 (7), 5.

Ji, K., Choi, K., 2013. Endocrine disruption potentials of bisphenol A alternatives - are bisphenol A alternatives safe from endocrine disruption? Korean J. Environ. Health Sci. 39, 1–18.

König, M., Escher, B.I., Neale, P.A., Krauss, M., Hilscherová, K., Novák, J., Teodorović, I., Schulze, T., Seidensticker, S., Kamal Hashmi, M.A., Ahlheim, J., Brack, W., 2017. Impact of untreated wastewater on a major European river evaluated with a combination of in vitro bioassays and chemical analysis. Environ. Pollut. 220, 1220–1230.

Kratochvil, I., Hofmann, T., Rother, S., Schlichting, R., Moretti, R., Scharnweber, D., Hintze, V., Escher, B.I., Meiler, J., Kalkhof, S., von Bergen, M., 2018. Mono(2-ethylhexyl) phthalate (MEHP) and mono(2-ethyl-5-oxohexyl) phthalate (MEOHP) but not di(2-ethylhexyl) phthalate (DEHP) bind productively to the peroxisome proliferator-activated receptor gamma. Rapid Commun. Mass Spectrom.

Le Magueresse-Battistoni, B., Labaronne, E., Vidal, H., Naville, D., 2017. Endocrine disrupting chemicals in mixture and obesity, diabetes and related metabolic disorders. World J. Biol. Chem. 8, 108–119.

Lefterova, M.I., Haakonsson, A.K., Lazar, M.A., Mandrup, S., 2014. PPARgamma and the global map of adipogenesis and beyond. Trends Endocrinol. Metab. 25, 293–302.

Legeay, S., Faure, S., 2017. Is bisphenol A an environmental obesogen? Fundam. Clin. Pharmacol. 31, 594–609.

Li, X., Fang, P., Mai, J., Choi, E.T., Wang, H., Yang, X.F., 2013. Targeting mitochondrial reactive oxygen species as novel therapy for inflammatory diseases and cancers. J. Hematol. Oncol. 6, 19.

Lo, K.A., Labadorf, A., Kennedy, N.J., Han, M.S., Yap, Y.S., Matthews, B., Xin, X., Sun, L., Davis, R.J., Lodish, H.F., Fraenkel, E., 2013. Analysis of in vitro insulin-resistance models and their physiological relevance to in vivo diet-induced adipose insulin resistance. Cell. Rep. 5, 259–270.

Longo, M., Zatterale, F., Naderi, J., Parrillo, L., Formisano, P., Raciti, G.A., Beguinot, F., Miele, C., 2019. Adipose tissue dysfunction as determinant of obesity-associated metabolic complications. Int. J. Mol. Sci. 20.

Manning, B.D., Toker, A., 2017. AKT/PKB signaling: navigating the network. Cell 169, 381–405.

Martinez, M.A., Blanco, J., Rovira, J., Kumar, V., Domingo, J.L., Schuhmacher, M., 2020. Bisphenol A analogues (BPS and BPF) present a greater obesogenic capacity in 3T3-L1 cell line. Food Chem. Toxicol. 140, 111298.

Masuno, H., Iwanami, J., Kidani, T., Sakayama, K., Honda, K., 2005. Bisphenol a accelerates terminal differentiation of 3T3-L1 cells into adipocytes through the phosphatidylinositol 3-kinase pathway. Toxicol. Sci. 84, 319–327.

Matulewicz, N., Stefanowicz, M., Nikolajuk, A., Karczewska-Kupczewska, M., 2017. Markers of adipogenesis, but not inflammation, in adipose tissue are independently related to insulin sensitivity. J. Clin. Endocrinol. Metab. 102, 3040–3049.

Miyawaki, J., Sakayama, K., Kato, H., Yamamoto, H., Masuno, H., 2007. Perinatal and postnatal exposure to bisphenol A increases adipose tissue mass and serum cholesterol level in mice. J. Atheroscl. Thrombosis 14, 245–252.

Moseti, D., Regassa, A., Kim, W.K., 2016. Molecular regulation of adipogenesis and potential anti-adipogenic bioactive molecules. Int. J. Mol. Sci. 17.

Nakachi, Y., Yagi, K., Nikaido, I., Bono, H., Tonouchi, M., Schonbach, C., Okazaki, Y., 2008. Identification of novel PPARgamma target genes by integrated analysis of ChIP-on-chip and microarray expression data during adipocyte differentiation. Biochem. Biophys. Res. Commun. 372, 362–366.

Nan, X., 2018. ggsci: scientific journal and Sci-Fi themed color palettes for 'ggplot2. R package version 2, 9.

Neale, P.A., Altenburger, R., Ait-Aissa, S., Brion, F., Busch, W., de Aragao Umbuzeiro, G., Denison, M.S., Du Pasquier, D., Hilscherova, K., Hollert, H., Morales, D.A., Novak, J., Schlichting, R., Seiler, T.B., Serra, H., Shao, Y., Tindall, A.J., Tollefsen, K.E., Williams, T.D., Escher, B.I., 2017. Development of a bioanalytical test battery for water quality monitoring: fingerprinting identified micropollutants and their contribution to effects in surface water. Water Res. 123, 734–750.

Neale, P.A., Leusch, F.D., 2015. Considerations when assessing antagonism in vitro: why standardizing the agonist concentration matters. Chemosphere 135, 20–23.

Ohlstein, J.F., Strong, A.L., McLachlan, J.A., Gimble, J.M., Burow, M.E., Bunnell, B.A., 2014. Bisphenol A enhances adipogenic differentiation of human adipose stromal/stem cells. J. Mol. Endocrinol. 53, 345–353.

Perez-Riverol, Y., Csordas, A., Bai, J., Bernal-Llinares, M., Hewapathirana, S., Kundu, D. J., Inuganti, A., Griss, J., Mayer, G., Eisenacher, M., Pérez, E., Uszkoreit, J., Pfeuffer, J., Sachsenberg, T., Yilmaz, S., Tiwary, S., Cox, J., Audain, E., Walzer, M., Jarnuczak, A.F., Ternent, T., Brazma, A., Vizcaíno, J.A., 2019. The PRIDE database and related tools and resources in 2019: improving support for quantification data. Nucleic Acids Res. 47, D442–D450.

Ritchie, M.E., Phipson, B., Wu, D., Hu, Y., Law, C.W., Shi, W., Smyth, G.K., 2015. limma powers differential expression analyses for RNA-sequencing and microarray studies. Nucleic. Acids Res. 43, e47.

Riu, A., Grimaldi, M., le Maire, A., Bey, G., Phillips, K., Boulahtouf, A., Perdu, E., Zalko, D., Bourguet, W., Balaguer, P., 2011. Peroxisome proliferator-activated receptor gamma is a target for halogenated analogs of bisphenol A. Environ. Health Perspect. 119, 1227–1232.

Rohart, F., Gautier, B., Singh, A., Lê Cao, K., 2017. mixOmics: An R package for 'omics feature selection and multiple data integration. PLoS Comput. Biol. 13, e1005752.

Sartipy, P., Loskutoff, D.J., 2003. Monocyte chemoattractant protein 1 in obesity and insulin resistance. Proc. Natl. Acad. Sci. U S A 100, 7265–7270.

Schmidt, J.R., Geurtzen, K., von Bergen, M., Schubert, K., Knopf, F., 2019. Glucocorticoid treatment leads to aberrant ion and macromolecular transport in regenerating zebrafish fins. Front. Endocrinol. (Lausanne) 10, 674.

Sell, H., Eckel, J., 2007. Monocyte chemotactic protein-1 and its role in insulin resistance. Curr. Opin. Lipidol. 18, 258–262.

Shang, J., Kojetin, D.J., 2021. Structural mechanism underlying ligand binding and activation of PPARγ. Structure. https://doi.org/10.1016/j.str.2021.02.006.

Sledzinski, T., Korczynska, J., Goyke, E., Stefaniak, T., Proczko-Markuszewska, M., Kaska, L., Swierczynski, J., 2013. Association between cytosolic glycerol 3-phosphate dehydrogenase gene expression in human subcutaneous adipose tissue and BMI. Cell Physiol. Biochem. 32, 300–309.

Song, S., Zhang, L., Zhang, H., Wei, W., Jia, L., 2014. Perinatal BPA exposure induces hyperglycemia, oxidative stress and decreased adiponectin production in later life of male rat offspring. Int. J. Environ. Res. Public Health 11, 3728–3742.

Stephen, T., 2019. Tmisc: Turner Miscellaneous. R package version (1), 22.

Straub, L.G., Scherer, P.E., 2019. Metabolic messengers: adiponectin. Nat. Metab. 1, 334–339.

Sun, Q., Li, J., Gao, F., 2014. New insights into insulin: The anti-inflammatory effect and its clinical relevance. World J. Diabetes 5, 89–96.

Tchkonia, T., Giorgadze, N., Pirtskhalava, T., Tchoukalova, Y., Karagiannides, I., Forse, R.A., DePonte, M., Stevenson, M., Guo, W., Han, J., Waloga, G., Lash, T.L., Jensen, M.D., Kirkland, J.L., 2002. Fat depot origin affects adipogenesis in primary cultured and cloned human preadipocytes. Am. J. Physiol. Regul. Integr. Comp. Physiol. 282, R1286–R1296.

Thoene, M., Dzika, E., Gonkowski, S., Wojtkiewicz, J., 2020. Bisphenol S in food causes hormonal and obesogenic effects comparable to or worse than bisphenol A: a literature review. Nutrients 12.

Tindall, C.A., Erkner, E., Stichel, J., Beck-Sickinger, A.G., Hoffmann, A., Weiner, J., Heiker, J.T., 2021. Cleavage of the vaspin N-terminus releases cell-penetrating peptides that affect early stages of adipogenesis and inhibit lipolysis in mature adipocytes. Adipocyte 10, 216–231.

Tontonoz, P., Hu, E., Graves, R.A., Budavari, A.I., Spiegelman, B.M., 1994. mPPAR gamma 2: tissue-specific regulator of an adipocyte enhancer. Genes Dev 8, 1224–1234.

Valentino, R., D'Esposito, V., Passaretti, F., Liotti, A., Cabaro, S., Longo, M., Perruolo, G., Oriente, F., Beguinot, F., Formisano, P., 2013. Bisphenol-A impairs insulin action and up-regulates inflammatory pathways in human subcutaneous adipocytes and 3T3-L1 cells. PLoS ONE 8, e82099.

van Marrewijk, L.M., Polyak, S.W., Hijnen, M., Kuruvilla, D., Chang, M.R., Shin, Y., Kamenecka, T.M., Griffin, P.R., Bruning, J.B., 2016. SR2067 reveals a unique kinetic

and structural signature for PPARgamma Partial Agonism. ACS Chem. Biol. 11 (1), 273–283. https://doi.org/10.1021/acschembio.5b00580.
Vandenberg, L.N., 2014. Non-monotonic dose responses in studies of endocrine disrupting chemicals: bisphenol a as a case study. Dose Response 12, 259–276.
Veiga-Lopez, A., Pennathur, S., Kannan, K., Patisaul, H.B., Dolinoy, D.C., Zeng, L., Padmanabhan, V., 2015. Impact of gestational bisphenol A on oxidative stress and free fatty acids: Human association and interspecies animal testing studies. Endocrinology 156, 911–922.
Vnukov, V.V., Gutsenko, O.I., Milyutina, N.P., Kornienko, I.V., Ananyan, A.A., Plotnikov, A.A., Panina, S.B., 2017. SkQ1 regulates expression of Nrf2, ARE-controlled genes encoding antioxidant enzymes, and their activity in cerebral cortex under oxidative stress. Biochemistry (Mosc) 82, 942–952.
Wabitsch, M., Brenner, R.E., Melzner, I., Braun, M., Moller, P., Heinze, E., Debatin, K.M., Hauner, H., 2001. Characterization of a human preadipocyte cell strain with high capacity for adipose differentiation. Int. J. Obes. Relat. Metab. Disord. 25, 8–15.
Wang, W., Zhang, X., Wang, Z., Qin, J., Wang, W., Tian, H., Ru, S., 2018. Bisphenol S induces obesogenic effects through deregulating lipid metabolism in zebrafish (Danio rerio) larvae. Chemosphere 199, 286–296.
Wang, Z., Karkossa, I., Grosskopf, H., Rolle-Kampczyk, U., Hackermuller, J., von Bergen, M., Schubert, K., 2020. Comparison of quantitation methods in proteomics to define relevant toxicological information on AhR activation of HepG2 cells by BaP. Toxicology 152652.
Wei, J., Lin, Y., Li, Y., Ying, C., Chen, J., Song, L., Zhou, Z., Lv, Z., Xia, W., Chen, X., Xu, S., 2011. Perinatal exposure to bisphenol A at reference dose predisposes offspring to metabolic syndrome in adult rats on a high-fat diet. Endocrinology 152, 3049–3061.
WHO, World Health Organization. 2020. https://www.who.int/news-room/fact-sheets/detail/obesity-and-overweight.
Wickham, H., 2007. Reshaping Data with thereshapePackage. J. Stat. Softw. 21.
Wickham, H., 2011. The split-apply-combine strategy for data analysis. J. Stat. Softw. 40.
Wickham, H., 2016. ggplot2: Elegant Graphics for Data Analysis. Springer-Verlag, New York.
Wickham, H., 2019. tidyr: Tidy Messy Data. R package version 1.
Wickham, H., Bryan, J., 2019. readxl: Read Excel Files. R package version 1 (3), 1.
Xin, F., Jiang, L., Liu, X., Geng, C., Wang, W., Zhong, L., Yang, G., Chen, M., 2014. Bisphenol A induces oxidative stress-associated DNA damage in INS-1 cells. Mutat. Res. Genet. Toxicol. Environ. Mutagen. 769, 29–33.
Yang, J., Wang, H., Du, H., Xu, L., Liu, S., Yi, J., Chen, Y., Jiang, Q., He, G., 2020. Serum Bisphenol A, glucose homeostasis, and gestational diabetes mellitus in Chinese pregnant women: a prospective study. Environ. Sci. Pollut. Res. Int.
Yang, X., Jansson, P.A., Nagaev, I., Jack, M.M., Carvalho, E., Sunnerhagen, K.S., Cam, M. C., Cushman, S.W., Smith, U., 2004. Evidence of impaired adipogenesis in insulin resistance. Biochem. Biophys. Res. Commun. 317, 1045–1051.
Yu, C., Chen, L., Luo, H., Chen, J., Cheng, F., Gui, C., Zhang, R., Shen, J., Chen, K., Jiang, H., Shen, X., 2004. 'Binding analyses between Human PPARgamma-LBD and ligands Surface plasmon resonance biosensor assay correlating with circular dichroic spectroscopy determination and molecular docking. Eur. J. Biochem. 271, 386–397.
Yuk, J.S., Hong, D.G., Jung, J.W., Jung, S.H., Kim, H.S., Han, J.A., Kim, Y.M., Ha, K.S., 2006. Sensitivity enhancement of spectral surface plasmon resonance biosensors for the analysis of protein arrays. Eur. Biophys. J. 35, 469–476.
Zhang, X., Smits, A.H., van Tilburg, G.B., Ovaa, H., Huber, W., Vermeulen, M., 2018. Proteome-wide identification of ubiquitin interactions using UbIA-MS. Nat. Protoc. 13, 530–550.
Ziemke, F., Mantzoros, C.S., 2010. Adiponectin in insulin resistance: lessons from translational research. Am. J. Clin. Nutr. 91, 258S–261S.
Zuo, H., Shi, Z., Yuan, B., Dai, Y., Wu, G., Hussain, A., 2013. Association between serum leptin concentrations and insulin resistance: a population-based study from China. PLoS ONE 8, e54615.
Zwick, R.K., Guerrero-Juarez, C.F., Horsley, V., Plikus, M.V., 2018. Anatomical, physiological, and functional diversity of adipose tissue. Cell Metab 27, 68–83.
Escher, B.I., Glauch, L., König, M., Mayer, P., Schlichting, R., 2019. Baseline toxicity and volatility cutoff in reporter gene assays used for high-throughput screening. Chem. Res. Toxicol. 32, 1646–1655.